Evolutionary suicide in a two-prey-one-predator model with Holling type II functional response

Caterina Vitale

Department of Mathematics and Statistics
Faculty of Science
University of Helsinki

May 2016

Contents

1 Introduction

This project started from Matsuda and Abrams paper: "Timid Consumers: Self-Extinction Due to Adaptive Change in Foraging and Anti-predator Effort". Matsuda and Abrams analyse the outcomes of prey timidity evolution in a prey-predator model with two different assumptions on predator dynamics. Prey timidity refers to the prey attitude of hiding from predators at the cost of less food intake and reduced possibility of reproduction. The indicator for prey timidity is the prey foraging effort. Low foraging effort indicates high prey timidity and vice versa. Matsuda and Abrams analyse two cases of predator dynamics: when predator population size is kept constant and when predator feeding depends exclusively upon prey abundance. In the latter case, natural selection favours the increase of prey timidity and causes the gradual disappearing of predator population due to the rarity of preys. While, for large values of fixed predator population size, the timidity increase caused by natural selection leads to the catastrophic extinction of the prey population itself. Although Matsuda and Abrams refer to this result as "self-extinction", we will use the terminology "evolutionary suicide", that was not yet introduced in 1994. More details on evolutionary suicide are in subsection 1.1. The choice of the functional response, i.e. the number of prey captured from one predator per unit of time, is crucial to obtain the evolutionary suicide. Matsuda and Abrams use an Holling type II functional response, which derivation and interpretation can be found in subsection 1.2. The first step of our project has been to reformulate Matsuda and Abrams' paper in the contest of Adaptive Dynamics [6], [3]. The same conclusions of the original paper can be drawn in the Adaptive Dynamics framework (subsection 1.4).

The idea of this thesis is to consider a more realistic choice of predator dynamics and investigate whether evolutionary suicide may still occur. More precisely, we introduce in the model a second type of prey with the assumption that the two types of prey are spatially separated. The reason of this assumption is explained in subsection 1.4. A general introduction on two-prey-one-predator system and effects of adaptive anti-predator behaviour can be found in [1].

In section 2 we analyse the two-prey-one-predator model under the assumption that the conversion rate of the first type of prey is equal to zero. In this case, predators still hunt the first type of prey either as snack or for entertainment without gaining any energy out of it. Under this assumption, our model reproduces Matsuda and Abrams' results both qualitatively and quantitatively. Moreover, we show that the introduction of the second type of prey allows the appearance of cycling behaviour in the solutions. Furthermore, we show an example where evolutionary suicide occurs on limit cycles. Section 2 ends with critical function analysis. Namely, we derive the conditions on the birth rate as function of prey foraging effort to obtain evolutionary suicide.

In section 3 we analyse the full model without simplifying assumptions. Because of the analytical complexity of the system we use numerical bifurcation analysis to study bifurcations of the internal equilibria. In this way, we are able to estimate the range for the first type of prey conversion rate where the results of Matsuda and Abrams' model hold.

1.1 Evolutionary suicide

In 1968 Garrett Hardin published a paper called "The Tragedy of the Commons" [9]. The name "tragedy of the commons" refers to an imaginary situation ideated by William Forster Lloyd to criticise the opinion that every rational man that acts for his own good favours also the common good. The scenario pictures a common field shared by the herdsmen of a community. The problem arises when a herdsman has to decide whether it is a good idea to introduce a new animal in

the field. The income produced by the new animal will advantage only the owner while the costs of grass consumption will be shared between all the herdsman. Thus, at the individual level the choice of increasing the number of animals in the common field is the best one. However, if all the herdsman adopt this behaviour the number of animals will increases until the point where the finite resources of the common field are completely exploited. The same choice that maximizes the individual benefit endangers the whole population. This is the concept behind evolutionary suicide, even though Hardin did not use this terminology. The name "evolutionary suicide" has been introduced in the framework of evolutionary conservation biology by Ferrière (2000). Ferrière used this term to describe the eventual extinction due to adaptive response of dispersal to habitat loss in a metapopulation. In this case, the fittest dispersal trait in the untouched habitat leads to extinction under the environmental change. We can find the biological formulation of evolutionary suicide in [5]:

> "Evolutionary suicide is defined as a trait substitution sequence driven by mutation and selection that takes a population toward and across a boundary in the population's trait space beyond which the population cannot persist."

Moreover, [5] distinguish between the process of evolutionary deterioration and evolutionary suicide. In the former, the evolution of a trait lowers the population density value to the point where extinction may occurs due to demographic or environmental stochasticity. While in the latter extinction occurs through a discontinuous transition. The mathematical modelling of this idea is provided in [8] and [7]. Gyllenberg *et al.* (2002) prove that a discontinuous transition to extinction, more precisely a catastrophic bifurcation, is a necessary but not sufficient condition to obtain evolutionary suicide in a structured metapopulation model when dispersal evolve. In particular, they prove that the extinction boundary is repelling when approached continuously. Furthermore, Gyllenberg and Parvinen (2002) derive necessary and sufficient conditions for a catastrophic bifurcation to shows evolutionary suicide in the larger framework of adaptive dynamics. Gyllenberg and Parvinen also present an example of evolutionary suicide due to asymmetric competition and Allee effect. In particular, the increasing of competitive traits like body size or length of horns is the most convenient choice at the individual level but it may drive the population to extinction due to reduced fertility. A detailed overview on evolutionary suicide can be found in Parviven (2005).

1.2 The Rosenzweig-McArthur model

The Rosenzweig-MacArthur model is an extension of the classical Lotka-Volterra prey-predator model [2]. The differences between the two models are in the predator-free dynamics and in the predator functional response. The predator-free dynamics is the dynamics of the prey population in absence of predators. In the Rosenzweig-MacArthur model the predator-free dynamics of the prey is logistic rather the exponential as in the Lotka-Volterra model. With predator functional response we refers to the number of prey captured from one predator per unit of time. In the Lokta-Volterra model the predator functional response is a linear function of the prey density. This assumption does not hold in the Rosenzweig-MacArthur model. As we said, when the predator population is not present the dynamics of the prey is logistic:

$$\frac{dn}{dt} = r\left(1 - \frac{n}{K}\right)n$$

where n is the prey density, r is the intrinsic growth rate, and K is the environmental carrying capacity. Later, we will use the logistic equation in this form

$$\frac{dn}{dt} = (B - d)n - \delta n^2.$$

with B per capita birth rate, d death rate, and δ competition rate. The two forms are equivalent with the parameter change:

$$r = B - d$$
$$K = \frac{(B - d)}{\delta}.$$

We can write the for prey (n) and predator (p) densities in the general form

$$\frac{dn}{dt} = r\left(1 - \frac{n}{K}\right)n - f(n)p$$
$$\frac{dp}{dt} = (\alpha f(n) - \epsilon)\, p,$$

where $f(n)$ is the predator functional response and ϵ the predator death rate. α is the conversion rate, i.e. the amount of preys that a predator needs to eat to be able to reproduce. The choice for $f(n)$ is the Holling type II functional response. To better interpret this functional response it is useful to go through its derivation. We will follow the one given by Éva Kisdi in the course *Introduction to Mathematical Biology*, Autumn 2015. To derive the Holling type II functional response we consider the predator population divided into two groups: the group of predators that is hunting and searching for a prey (p_s) and the group of predators that is handling the prey (p_h). The total predator density can be written as $p(t) = p_s(t) + p_h(t)$. With this distinction only searching predators contribute to the prey capture. Furthermore, we assume that the time scale at which hunting and handling happen is considerably faster than the time scale of predator and prey birth and death. These assumptions allow us to perform a time scale separation between the slow population dynamics of n and p and the fast transitions between searching and handling. At the fast time scale n and p can be considered constant $(\bar{n}, \bar{p})$, since their dynamics are slow enough to be not noticeable. The transitions between the state of searching (S) and the state of handling (H) are

$$\text{(S)} \xrightarrow{\beta\bar{n}} \text{(H)}$$
$$\text{(H)} \xrightarrow{1/h} \text{(S)}$$

with β capture rate and h constant handling time. Thus the system for the two types of predator is

$$\frac{dp_s}{dt} = -\beta\bar{n}p_s + \frac{1}{h}p_h$$
$$\frac{dp_h}{dt} = +\beta\bar{n}p_s - \frac{1}{h}p_h$$

By substituting $p_h = \bar{p} - p_s$ we can reduce the system at the equation for p_s alone,

$$\frac{dp_s}{dt} = \frac{1}{h}\bar{p} - \left(\beta\bar{n} + \frac{1}{h}\right) p_s. \tag{1}$$

The quasi-equilibrium

$$\bar{p}_s = \frac{\bar{p}}{1 + h\beta\bar{n}}$$

is globally asymptotically stable stable since the derivative of the left-hand side of (1) with respect to p_s is negative. Note that $\bar{p}_s$ represents the fraction of searching predators at the equilibrium of the searching-handling dynamics. We can now come back at the slow time scale. At this time scale the transitions between handling and searching are fast enough to constantly reach the quasi-equilibrium

$$\bar{p}_s = \frac{p}{1 + h\beta n}.$$

By reminding that only searching predators contribute to prey capture, we can write the system for prey and predator densities as

$$\begin{aligned} \frac{dn}{dt} &= r\left(1 - \frac{n}{K}\right) - \beta n \bar{p}_s \\ \frac{dp}{dt} &= \alpha\beta n\bar{p}_s - \epsilon p, \end{aligned}$$

that can be rewritten as

$$\begin{aligned} \frac{dn}{dt} &= r\left(1 - \frac{n}{K}\right) - \frac{\beta np}{1 + h\beta n} \\ \frac{dp}{dt} &= \frac{\alpha\beta np}{1 + h\beta n} - \epsilon p. \end{aligned} \tag{2}$$

Model (2) is the Rosenzweig-MacArthur model and

$$f(n) = \frac{\beta n}{1 + h\beta n}$$

is the Holling type II functional response.

1.3 Matsuda and Abrams' model

Matsuda and Abrams in [11] analyse a prey-predator system where prey timidity is assumed to evolve. Two cases are considered: when predator density is fixed and when predator reproduction rate depends upon prey density. In the former case prey dynamics is determined by the equation:

$$\frac{dn}{dt} = \left(\frac{c}{1 + bc} - d - \delta n - \frac{c\bar{p}}{1 + chn}\right) n$$

where

$$
\begin{aligned}
n &= \text{prey density} \\
\bar{p} &= \text{constant predator density} \\
c &= \text{prey foraging effort} \\
\frac{1}{b} &= \text{asymptotic saturation value of the benefit got from resource intake} \\
B(c) &:= \frac{c}{1+bc} = \text{prey birth rate} \\
d &= \text{prey death rate} \\
\delta &= \text{prey competition rate} \\
h &= \text{predator handling time.}
\end{aligned}
$$

Note that the birth rate depends upon the foraging effort c. In particular, $B(c)$ is increasing with respect to c and it saturates at the limit value $1/b$. Another important assumption is the Holling type II predator functional response. The system shows three equilibria: the trivial one and the two roots of

$$\frac{c}{1+bc} - d - \delta n - \frac{c\bar{p}}{1+chn} = 0.$$

The largest root is always a stable equilibrium when it is real and positive. Analogously the smaller one is an unstable equilibrium when it's real and positive.

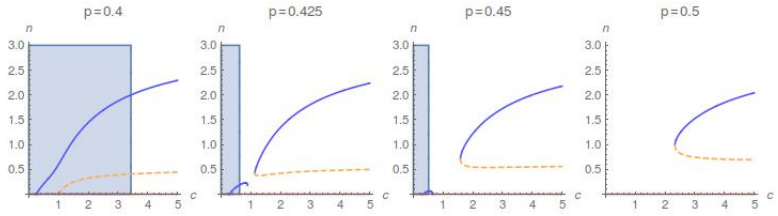

Figure 1: Plot of the not-trivial equilibria as function of the foraging effort for constant values of predator density. The blue line is for stable equilibria, the orange dashed line is for unstable equilibria. In the blue region the selection gradient is positive. $b = 1, d = 0.1, \delta = 0.25, h = 1, g = 0.1$.

Assuming that the population is at the positive stable equilibrium, we consider the case where a mutant with a slightly different foraging effort appears in the population. In such a case the equation for the mutant dynamics is:

$$\frac{dm}{dt} = \left(-d - \delta\bar{n} + \frac{k}{1+bk} - \frac{k\bar{p}}{1+hc\bar{n}}\right) m$$

where k is the mutant foraging effort and $\bar{n}$ the prey stable equilibrium. Note that the predator functional response still depends upon c, since the predation rate is determined by the resident population or, as stated in Matsuda and Abrams' paper, by the average value of foraging effort in prey population. The evolutionary result can be seen in the PIP.

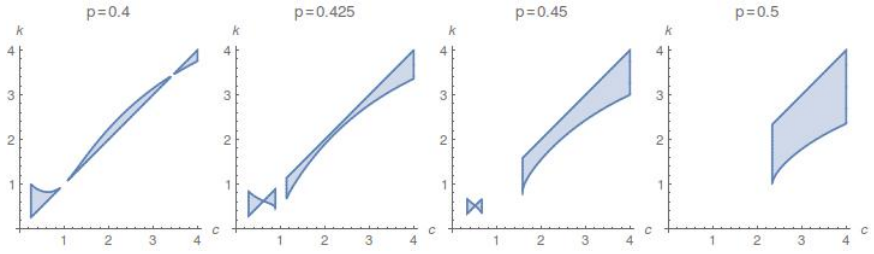

Figure 2: Pairwise invasibility plot for constant predator density. In the blue region the invasion fitness is positive. $b = 1, d = 0.1, \delta = 0.25, h = 1, g = 0.1$.

When predator density is low, mutants with an higher foraging effort can invade until the birth rate saturate and there is any more advantages in increasing c. When predator density is high, selection favours mutants with less foraging effort until the population can not reproduce enough to survive. The system behaviour is significantly different if the predator birth rate depends on the prey density. System equations are:

$$\frac{dn}{dt} = \left(-d - \delta n + \frac{c}{1+bc} - \frac{cp}{1+hcn}\right) n$$
$$\frac{dp}{dt} = \left(-\epsilon + \frac{\alpha cn}{1+hcn}\right) p,$$

with ϵ predator death rate and α predator conversion rate. The equilibrium value for n is

$$\bar{n} = \frac{\epsilon}{c(\alpha - \epsilon h)}.$$

Thus, it is no longer possible that an evolutionary suicide may occur. When the prey foraging effort becomes smaller predator population goes extinct before the prey one.

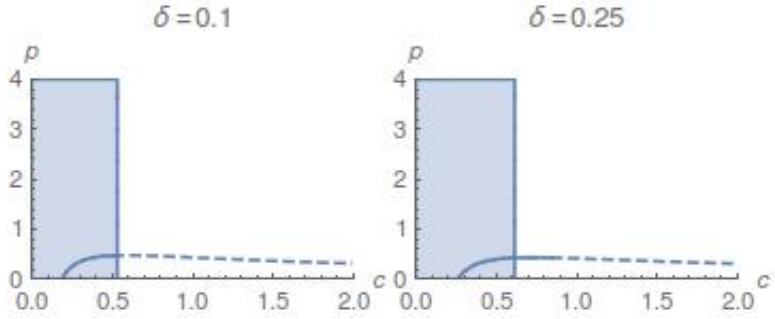

Figure 3: Plot of $\bar{n}$ for different values of prey competition rate. The continuous line indicates that $\bar{n}$ is stable, the dashed line indicates that $\bar{n}$ is unstable.In the blue region the selection gradient is positive. $\alpha = 1, b = 1, d = 0.1, h = 1, \epsilon = 0.1, g = 0.1$.

Evolution leads in this case to an ESS that can be either an equilibrium or a cycle.

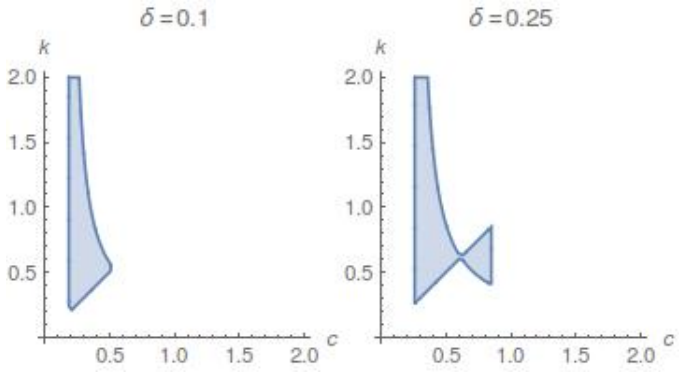

Figure 4: Pairwise invasibility plot for variable predator density. In the blue region the invasion fitness is positive. $\alpha = 1, b = 1, d = 0.1, h = 1, \epsilon = 0.1, g = 0.1$.

1.4 First attempt

First idea was to introduce in the system a new prey with same dynamics of the first one but different parameters:

$$\begin{aligned}
\frac{dn_1}{dt} &= \left(-d_1 - \delta_1 n_1 + \frac{\rho_1 c_1}{1+\rho_1 b_1 c_1} - \frac{\beta_1 c_1 p}{1 + h_1\beta_1 c_1 n_1 + h_2\beta_2 c_2 n_2}\right) n_1 \\
\frac{dn_2}{dt} &= \left(-d_2 - \delta_2 n_2 + \frac{\rho_2 c_2}{1+\rho_2 b_2 c_2} - \frac{\beta_2 c_2 p}{1 + h_1\beta_1 c_1 n_1 + h_2\beta_2 c_2 n_2}\right) n_2 \\
\frac{dp}{dt} &= \left(-\epsilon + \frac{\alpha_1\beta_1 c_1 n_1 + \alpha_2\beta_2 c_2 n_2}{1 + h_1\beta_1 c_1 n_1 + h_2\beta_2 c_2 n_2}\right) p
\end{aligned}$$

with β_i, $i = 1, 2$, predators attack rates. Let's define $B_i(c) = \rho_i c/(1 + \rho_i b_i c)$ as the non linear birth rate as function of c. The parameters ρ_i have been introduced to control the slope of the birth rate at the origin. To find a non trivial equilibrium we need to solve the system

$$0 = -d_1 - \delta_1 n_1 + \frac{\rho_1 c_1}{1+\rho_1 b_1 c_1} - \frac{\beta_1 c_1 p}{1 + h_1\beta_1 c_1 n_1 + h_2\beta_2 c_2 n_2} \tag{3}$$

$$0 = -d_2 - \delta_2 n_2 + \frac{\rho_2 c_2}{1+\rho_2 b_2 c_2} - \frac{\beta_2 c_2 p}{1 + h_1\beta_1 c_1 n_1 + h_2\beta_2 c_2 n_2} \tag{4}$$

$$0 = -\epsilon + \frac{\alpha_1\beta_1 c_1 n_1 + \alpha_2\beta_2 c_2 n_2}{1 + h_1\beta_1 c_1 n_1 + h_2\beta_2 c_2 n_2}. \tag{5}$$

From (3) we get

$$\frac{p}{1 + h_1\beta_1 c_1 n_1 + h_2\beta_2 c_2 n_2} = \frac{1}{\beta_1 c_1}\left(-d_1 - \delta_1 n_1 + \frac{\rho_1 c_1}{1+\rho_1 b_1 c_1}\right),$$

that means that the searching predator fraction is set at the equilibrium by prey density. By plugging in it into (4), we find the linear relation between n_1 and n_2:

$$-d_2 - \delta_2 n_2 + \frac{\rho_2 c_2}{1+\rho_2 b_2 c_2} = \frac{\beta_2 c_2}{\beta_1 c_1}\left(-d_1 - \delta_1 n_1 + \frac{\rho_1 c_1}{1+\rho_1 b_1 c_1}\right).$$

A second linear relation is given by (5)

$$(\alpha_1 - \epsilon h_1)c_1 n_1 = \epsilon - (\alpha_2 - \epsilon h_2)c_2 n_2.$$

Because of these linear relations this model can not show any fold bifurcation. Thus, it is not useful for the purposes of this project.

2 The limit model ($\alpha_1 = 0$)

One idea to overcome the problem previously discussed is to hypothesize that the two prey populations live in different habitats. Predators spend a fraction q of time in the first-type prey's habitat and a fraction $1 - q$ in the second-type prey's habitat. The equations for the three populations densities are

$$\begin{aligned}
\frac{dn_1}{dt} &= \left(-d_1 - \delta_1 n_1 + \frac{\rho_1 c_1}{1 + \rho_1 b_1 c_1} - \frac{q\beta_1 c_1 p}{1 + h_1 c_1 \beta_1 n_1}\right) n_1 \\
\frac{dn_2}{dt} &= \left(-d_2 - \delta_2 n_2 + \frac{\rho_2 c_2}{1 + \rho_2 b_2 c_2} - \frac{(1-q)\beta_2 c_2 p}{1 + h_2 c_2 \beta_2 n_2}\right) n_2 \\
\frac{dp}{dt} &= \left(-\epsilon + \frac{\alpha_1 q \beta_1 c_1 n_1}{1 + h_1 \beta_1 c_1 n_1} + \frac{\alpha_2 (1-q)\beta_2 c_2 n_2}{1 + h_2 \beta_2 c_2 n_2}\right) p.
\end{aligned}$$

Note that, when n_1 or n_2 are equal to zero, the model is the Rosenzweig-MacArthur model that we derive in subsection 1.2.

First step in the model analysis is to assume $\alpha_1 = 0$. This is not an intuitive or reasonable assumption since, in this case, predators waste a fraction q of their time hunting a prey that give no nutritional power. By letting q evolve, in the long term it would go to 0. However, this assumption allow us to reproduce the results of Matsuda and Abrams' model. Their model becomes the "limit model" when $\alpha_1 \to 0$. To simplify calculations we first analyse the case where also $h_2 = 0$.

2.1 Case $h_2 = 0$

By considering the assumptions $\alpha_1 = 0$ and $h_2 = 0$, the analysed system becomes

$$\begin{aligned}
\frac{dn_1}{dt} &= \left(-d_1 - \delta_1 n_1 + \frac{\rho_1 c_1}{1 + \rho_1 b_1 c_1} - \frac{q\beta_1 c_1 p}{1 + h_1 c_1 \beta_1 n_1}\right) n_1 \\
\frac{dn_2}{dt} &= \left(-d_2 - \delta_2 n_2 + \frac{\rho_2 c_2}{1 + \rho_2 b_2 c_2} - (1-q)\beta_2 c_2 p\right) n_2 \\
\frac{dp}{dt} &= \left(-\epsilon + \alpha_2 (1-q)\beta_2 c_2 n_2\right) p.
\end{aligned}$$

Trivial equilibria of the system and their properties are summarised in the following table:

Equilibrium	Positivity	Stability
$(0, 0, 0)$		$c_1 < c_1^0 \wedge c_2 < c_2^0$
$(n_1^0, 0, 0)$	$c_1 > c_1^0$	$c_2 < c_2^0$
$(0, n_2^0, 0)$	$c_2 > c_2^0$	$c_1 < c_1^0 \wedge c_2 < \tilde{c}_2$
$(n_1^0, n_2^0, 0)$	$c_1 > c_1^0 \wedge c_2 > c_2^0$	$c_2 < \tilde{c}_2$

where

$$\begin{aligned}
n_i^0 &= \frac{1}{\delta_i}\left(\frac{\rho_i c_i}{1 + \rho_i b_i c_i} - d_i\right) \\
c_i^0 &= \frac{d_i}{\rho_i (1 - b_i d_i)}, \text{ with } i = 1, 2
\end{aligned}$$

and

$$\tilde{c}_2 = \frac{(1-q)\alpha_2\beta_2 d_2 + \epsilon\delta_2\rho_2 b_2 + \sqrt{((1-q)\alpha_2\beta_2 d_2 + \epsilon\delta_2\rho_2 b_2)^2 + 4\epsilon\delta_2(1-q)\alpha_2\beta_2\rho_2 D_2}}{2(1-q)\alpha_2\beta_2\rho_2 D_2}.$$

Under the assumption that $D_i = 1 - d_i b_i > 0$, $i = 1, 2$, all the listed quantities are positive. The last boundary equilibrium is $(0, \bar{n}_2, \bar{p})$, with values

$$\bar{n}_2 = \frac{\epsilon}{(1-q)\alpha_2\beta_2 c_2}$$
$$\bar{p} = \frac{1}{\beta_2 c_2 (1-q)} \left(\frac{\rho_2 c_2}{1 + \rho_2 b_2 c_2} - d_2 - \delta_2 \bar{n}_2 \right).$$

$\bar{n}_2$ is always positive and $\bar{p}$ is positive when $c_2 > \tilde{c}_2$. To interpret this condition we can study the dynamics in the (n_2, p)-plane. This dynamics is not affected by the behaviour of n_1 because $\alpha_1 = 0$. We notice the transcritical bifurcation between the equilibria $(0, n_2^0, 0)$ and $(0, \bar{n}_2, \bar{p})$, that occurs

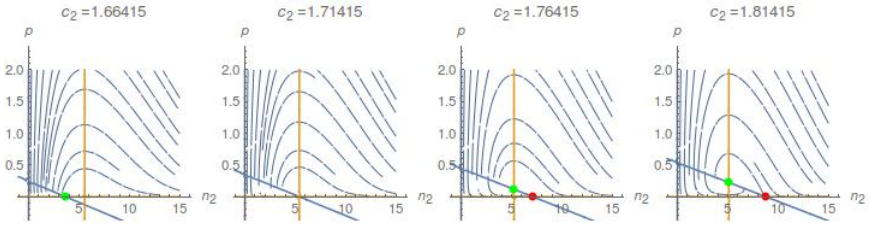

Figure 5: Dynamics in the (n_2, p)-plane when $h_2 = 0$.
$d_1 = 0.4$, $\delta_1 = 0.25$, $b_1 = 1$, $q = 0.9$, $h_1 = 1$, $\rho_1 = 1$, $\beta_1 = 1$, $d_2 = 0.9$, $\delta_2 = 0.01$, $b_2 = 0.4$, $\rho_2 = 0.9$, $\beta_2 = 0.9$, $\epsilon = 0.5$, $\alpha_2 = 0.6$.

when $c_2 = \tilde{c}_2$. The predator population is viable only when the second-type prey forages enough. The value of c_1 influences the stability of $(0, \bar{n}_2, \bar{p})$ in the 3D-space. More specifically, when the eigenvalue

$$\lambda_t = -d_1 + B_1(c_1) - q\beta_1 c_1 \bar{p} > 0,$$

$(0, \bar{n}_2, \bar{p})$ is transversally unstable. We need to study under which conditions $\lambda_t > 0$ to determine the transversal instability of $(0, \bar{n}_2, \bar{p})$. After substituting the value of $B_1(c_1) = \rho_1 c_1/(1 + \rho_1 b_1 c_1)$, and rearranging the terms for c_1,

$$\lambda_t = \frac{-q\rho_1\beta_1 b_1 \bar{p} c_1^2 + (D_1\rho_1 - q\beta_1\bar{p})c_1 - d_1}{1 + b_1\rho_1 c_1}.$$

λ_t assumes positive values when the parabola's vertex at the numerator is in the I quadrant. The vertex's abscissa is positive when

$$\bar{p} < \bar{p}_x = \frac{\rho_1 D_1}{q\beta_1}.$$

The vertex's ordinate is positive when

$$\bar{p} < \bar{p}_{y_1} = \frac{\rho_1}{q\beta_1}\left(1 - \sqrt{d_1 b_1}\right)^2 \vee \bar{p} > \bar{p}_{y_2} = \frac{\rho_1}{q\beta_1}\left(1 + \sqrt{d_1 b_1}\right)^2.$$

Considered that $\bar{p}_{y_1} < \bar{p}_x < \bar{p}_{y_2}$, when $\bar{p} < \bar{p}_{y_1}$ λ_t is positive for $c_1^- < c_1 < c_1^+$, with

$$c_1^{\pm} = \frac{\rho_1 D_1 - q\beta_1\bar{p} \pm \sqrt{(\rho_1 D_1 - q\beta_1\bar{p})^2 - 4qd_1\rho_1\beta_1 b_1\bar{p}}}{2q\rho_1\beta_1 b_1\bar{p}},$$

and $(0, \bar{n}_2, \bar{p})$ is unstable. In all other cases, $(0, \bar{n}_2, \bar{p})$ is transversally stable.

Let's now analyse the equilibrium $(\bar{n}_1, \bar{n}_2, \bar{p})$. Since $\alpha_1 = 0$, equations for n_2 and p are independent from n_1 and the equilibrium values for n_2 and p are the same as in $(0, \bar{n}_2, \bar{p})$, with the same condition for positivity $c_2 > \tilde{c}_2$. There are two possible equilibrium value for n_1:

$$\begin{aligned}
\bar{n}_1^{\pm} &= \frac{c_1\beta_1 h_1(B_1(c_1) - d_1) - \delta_1 \pm \sqrt{\Delta}}{2\delta_1 c_1\beta_1 h_1}, \\
\text{with } \Delta &= (c_1\beta_1 h_1(B_1(c_1) - d_1) - \delta_1)^2 + 4\delta_1 c_1\beta_1 h_1(B_1(c_1) - d_1 - q\beta_1 c_1\bar{p}) \\
&= (c_1\beta_1 h_1(B_1(c_1) - d_1) - \delta_1)^2 + 4\delta_1 c_1\beta_1 h_1\lambda_t.
\end{aligned}$$

To have any real solutions, Δ has to be not-negative. This happens when

$$\bar{p} \leq \frac{[c_1\beta_1 h_1(B_1(c_1) - d_1) + \delta_1]^2}{4q\delta_1\beta_1^2 h_1 c_1^2} = \bar{p}_{crit}. \tag{6}$$

Under this hypothesis, to have two positive roots we need that

$$\lambda_t < 0, \tag{7a}$$

$$c_1\beta_1 h_1(B_1(c_1) - d_1) - \delta_1 > 0. \tag{7b}$$

As discussed before, condition (7a) is satisfied for every $c_1 > 0$ if $\bar{p} > \bar{p}_{y_1}$, and for $c_1 < c_1^- \vee c_1 > c_1^+$ if $\bar{p} < \bar{p}_{y_1}$. Condition (7b) is satisfied when $c_1 > \tilde{c}_1$, with

$$\tilde{c}_1 = \frac{d_1\beta_1 h_1 + \rho_1\delta_1 b_1 + \sqrt{(d_1\beta_1 h_1 + \rho_1\delta_1 b_1)^2 + 4\delta_1\rho_1\beta_1 h_1 D_1}}{2\rho_1\beta_1 h_1 D_1}.$$

There are a positive root and a negative root when $\lambda_t > 0$. There are two negative roots when $c_1 < \tilde{c}_1 \wedge \lambda_t < 0$. Note that when the predator population is small enough, condition (6), n_1 can invade $(0, \bar{n}_2, \bar{p})$ for small initial values when $\lambda_t > 0$ and $(0, \bar{n}_2, \bar{p})$ is transversally unstable. However, it is also possible that the first-type species can be present at an internal equilibrium when $\lambda_t < 0$, precisely when condition (7b) is satisfy and the initial value is large enough. Moreover, $\bar{n}_1^+$ is always stable when it is real and positive and $\bar{n}_1^-$ is always unstable when it is real and positive. In the case where the $\Delta = 0$, meaning that $\bar{p} = \bar{p}_{crit}$, and $c_1 > \tilde{c}_1$ there is a positive multiple root with value

$$\bar{n}_1 = \frac{c_1\beta_1 h_1(B_1(c_1) - d_1) - \delta_1}{2\delta_1 c_1\beta_1 h_1} = \bar{n}_{crit}.$$

By choosing the parameter set

$$\begin{gathered}
d_1 = 0.1,\ \delta_1 = 0.25,\ b_1 = 1,\ \rho_1 = 1,\ \beta_1 = 1, h_1 = 1, \\
d_2 = 0.9,\ \delta_2 = 0.01,\ b_2 = 0.4,\ \rho_2 = 0.9,\ \beta_2 = 0.9,\ \alpha_2 = 0.6, \\
q = 0.9,\ \epsilon = 0.5,
\end{gathered} \tag{8}$$

the model shows the same results as Matsuda and Abrahms'one. Stability regions for the equilibria are summarized in Fig.6.

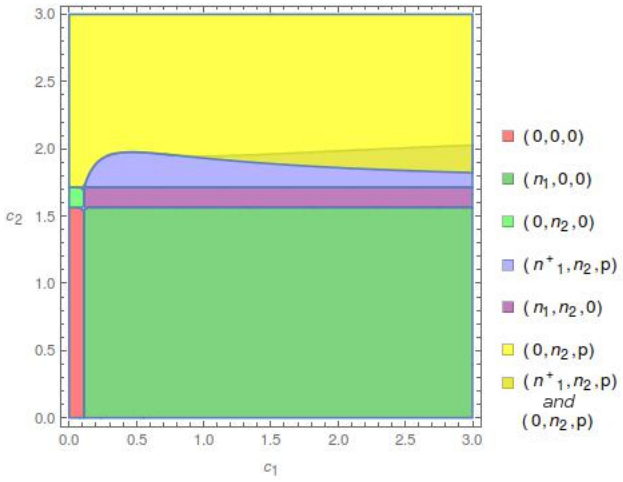

Figure 6: Summary of the stability regions of all equilibria when $h_2 = 0$ and $\alpha_1 = 0$. In the intersection between $(\bar{n}_1^+, \bar{n}_2, \bar{p})$ and $(0, \bar{n}_2, \bar{p})$ stability region (dark yellow), $\bar{n}_1^-$ is positive but the equilibrium is unstable.
$d_1 = 0.1$, $\delta_1 = 0.25$, $b_1 = 1$, $\rho_1 = 1$, $\beta_1 = 1, h_1 = 1$, $d_2 = 0.9$, $\delta_2 = 0.01$, $b_2 = 0.4$, $\rho_2 = 0.9$, $\beta_2 = 0.9$, $\alpha_2 = 0.6, q = 0.9$, $\epsilon = 0.5$.

In order to apply Adaptive Dynamics theory we rewrite $c_1 = x$, the resident foraging effort, and define

$$s_x(y) = -d_1 - \delta_1 \bar{n}_1^+ + \frac{\rho_1 y}{1 + \rho_1 b_1 y} - \frac{q\beta_1 y \bar{p}}{1 + h_1 \beta_1 x \bar{n}_1^+}$$

as the mutant invasion fitness, with y mutant strategy. Note that the system is assumed to be at the stable equilibrium $(\bar{n}_1^+, \bar{n}_2, \bar{p})$. Moreover, we define

$$[\partial_y s_x(y)]_{y=x} = \frac{\rho_1}{(1 + b_1 \rho_1 x)^2} - \frac{q\beta_1 \bar{p}}{1 + h_1 \beta_1 x \bar{n}_1^+}$$

as the selection gradient. In this system every attracting singular strategy is an ESS because

$$\left[\partial_y^2 s_x(y)\right]_{y=x} = -\frac{2 b_1 \rho_1^2}{(1 + b_1 \rho_1 x)^3} < 0, \quad \forall x > 0.$$

In Fig.7, we can see that $n_1^\pm$ as functions of c_1 have the same behaviour as in Matsuda and Abrams' model with the difference that now the predator density is set by c_2.

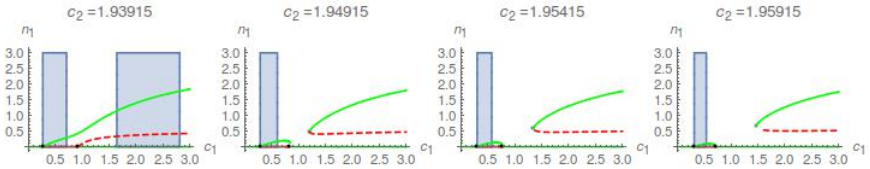

Figure 7: $\bar{n}_1^{\pm}$ as functions of c_1. Green line for $\bar{n}_1^{+}$, red and dashed line for $\bar{n}_1^{-}$. Where $\bar{n}_1^{+}$ is real and positive, the selection gradient is positive in the blue region and negative in the white one. $d_1 = 0.1$, $\delta_1 = 0.25$, $b_1 = 1$, $\rho_1 = 1$, $\beta_1 = 1, h_1 = 1$, $d_2 = 0.9$, $\delta_2 = 0.01$, $b_2 = 0.4$, $\rho_2 = 0.9$, $\beta_2 = 0.9$, $\alpha_2 = 0.6, q = 0.9$, $\epsilon = 0.5$.

We can see also in the pairwise invasibility plots in Fig.8 that this is an example of evolutionary suicide.

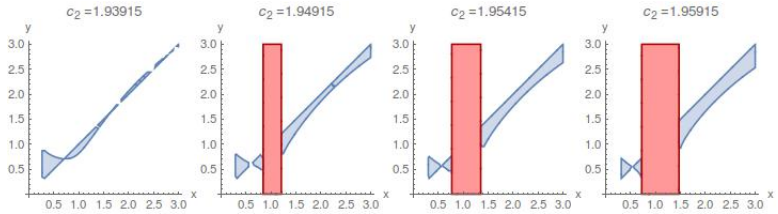

Figure 8: Pairwise invasibility plots for different values of c_2. In the red region $\bar{n}_1^{+}$ is complex and the blue region the invasion fitness is positive. $d_1 = 0.1$, $\delta_1 = 0.25$, $b_1 = 1$, $\rho_1 = 1$, $\beta_1 = 1, h_1 = 1$, $d_2 = 0.9$, $\delta_2 = 0.01$, $b_2 = 0.4$, $\rho_2 = 0.9$, $\beta_2 = 0.9$, $\alpha_2 = 0.6, q = 0.9$, $\epsilon = 0.5$.

Now, we want to investigate whether the evolutionary suicide is the only possible evolutionary outcome. This is not the case. In particular, we construct a case where the selection gradient is positive at the bifurcation point and the system evolves towards an evolutionary stable strategy on the equilibria branch of $\bar{n}_1^{+}$. First, let's define

$$g(x) = \frac{\rho_1}{(1 + b_1\rho_1 x)^2} - \frac{q\beta_1\bar{p}_{crit}}{1 + h_1\beta_1 x\bar{n}_{crit}}$$

as the selection gradient evaluated at $(\bar{n}_{crit}, \bar{p}_{crit})$. Note that, with this parameter set, $g(x)$ is negative for every value of x. Thus, evolution leads to extinction for choices of initial c_1 sufficiently high. The crucial observation is that $g(x)$ is independent of c_2, since $\bar{n}_{crit}$ and $\bar{p}_{crit}$ are functions of the first-type prey's parameters. This implies that we can set the parameters for the first-type prey to have $g(x) > 0$ and, then, find the value of c_2 such that $\bar{p} = \bar{p}_{crit}$. To look for the right parameter set for n_1 we plot $g(x)$ for different values of b_1 as in Fig.9. Once chosen the values x^* and b_1^* such that $g(x^*) > 0$, we compute $\bar{p}_{crit}$. We obtain the value for c_2 by solving $\bar{p} = \bar{p}_{crit}$. In Fig.10 it can be observed the transition between a case where $g(x)$ is positive, in the left panel, and the case where $g(x) < 0$ in the right panel. In all the panels $\bar{p}$ has been chosen such that the bifurcation point has the same coordinates. Remind that $1/b_1$ is the asymptotic value of the birth rate $B_1(c_1)$. Thus, a population with smaller b_1 reproduces faster than one with larger b_1 and the same foraging effort. When $b_1 = 0.5$ evolution pushes the population away from the bifurcation point, avoiding the evolutionary suicide. Since b_1 is small, increasing the foraging effort largely increases the reproduction rate. For this reason, the invasion fitness is positive for large c_1 even

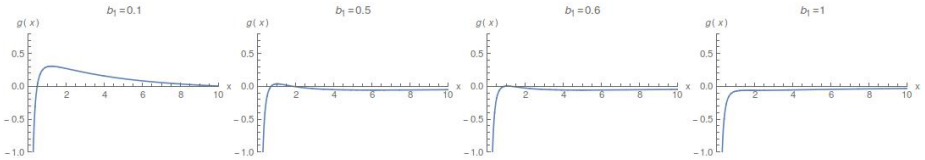

Figure 9: Selection gradient evaluated at $(\bar{n}_{crit}, \bar{p}_{crit})$ for different values of b_1. $d_1 = 0.1, \delta_1 = 0.25, q = 0.9, h_1 = 1, \rho_1 = 1, \beta_1 = 1, \epsilon = 0.5$.

though the predator density is higher than in the other panels. In the second panel, we have evolutionary suicide for a small range of initial c_1 close to the bifurcation point. For larger initial c_1 evolution leads to an evolutionary stable strategy. When the reproduction rate is close to saturate there are not any more advantages in increasing c_1. In the last two panels, we are back in the situation analysed in Fig.7 and Fig.8. Since the asymptotic value of the birth rate function is low, an increase in the foraging effort does not improve considerably the reproduction rate. Therefore, the selection gradient favours prey timidity and the system evolves through evolutionary suicide.

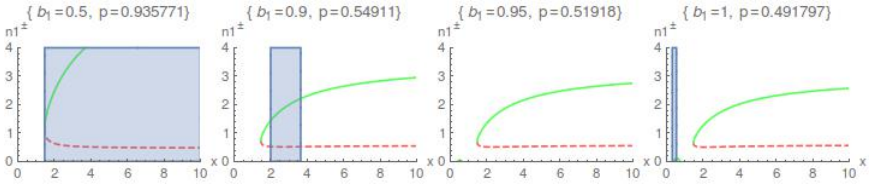

Figure 10: $\bar{n}_1^{\pm}$ as functions of c_1 for different values of b_1. Green line for $\bar{n}_1^{+}$, red and dashed line for $\bar{n}_1^{-}$. Where $\bar{n}_1^{+}$ is real and positive, the selection gradient is positive in the blue region and negative in the white one. $x^* = 1.47, d_1 = 0.1, \delta_1 = 0.25, q = 0.9, h_1 = 1, \rho_1 = 1, \beta_1 = 1, d_2 = 0.9, \delta_2 = 0.01, b_2 = 0.4, \rho_2 = 0.9, \beta_2 = 0.9, \epsilon = 0.5, \alpha_2 = 0.6$.

2.2 Case $h_2 \neq 0$

We now analyse

$$\begin{aligned}
\frac{dn_1}{dt} &= \left(-d_1 - \delta_1 n_1 + \frac{\rho_1 c_1}{1 + \rho_1 b_1 c_1} - \frac{q\beta_1 c_1 p}{1 + h_1 c_1 \beta_1 n_1}\right) n_1 \\
\frac{dn_2}{dt} &= \left(-d_2 - \delta_2 n_2 + \frac{\rho_2 c_2}{1 + \rho_2 b_2 c_2} - \frac{(1-q)\beta_2 c_2 p}{1 + h_2 \beta_2 c_2 n_2}\right) n_2 \\
\frac{dp}{dt} &= \left(-\epsilon + \frac{\alpha_2 (1-q)\beta_2 c_2 n_2}{1 + h_2 \beta_2 c_2 n_2}\right) p.
\end{aligned}$$

The behaviour of the trivial equilibria is qualitatively analogous to the previous case:

Equilibrium	Positivity	Stability
$(0,0,0)$		$c_1 < c_1^0 \wedge c_2 < c_2^0$
$(n_1^0, 0, 0)$	$c_1 > c_1^0$	$c_2 < c_2^0$
$(0, n_2^0, 0)$	$c_2 > c_2^0$	$c_1 < c_1^0 \wedge c_2 < \tilde{c}_2$
$(n_1^0, n_2^0, 0)$	$c_1 > c_1^0 \wedge c_2 > c_2^0$	$c_2 < \tilde{c}_2$

where

$$n_i^0 = \frac{1}{\delta_i}\left(\frac{\rho_i c_i}{1+\rho_i b_i c_i} - d_i\right)$$
$$c_i^0 = \frac{d_i}{\rho_i(1-b_i d_i)}, \text{ with } i = 1, 2$$
$$\tilde{c}_2 = \frac{d_2\beta_2 H_2 + \epsilon b_2\rho_2\delta_2 + \sqrt{(d_2\beta_2 H_2 + \epsilon b_2\rho_2\delta_2)^2 + 4\epsilon\delta_2\beta_2 H_2\rho_2 D_2}}{2\beta_2 H_2\rho_2 D_2}.$$

In the overlap between $(\bar{n}_1^+, \bar{n}_2, \bar{p})$ and $(0, \bar{n}_2, \bar{p})$ stability region, $\bar{n}_1^-$ is positive but the equilibrium is unstable. $H_2 = (1-q)\alpha_2 - h_2\epsilon$ and $D_i = 1 - d_i b_i$, $i = 1, 2$, are assumed to be positive. Again, it is useful to investigate the dynamics in the (n_2, p)-plane, since it is still independent from n_1. In this case the values of $(0, \bar{n}_2, \bar{p})$ are

$$\bar{n}_2 = \frac{\epsilon}{\beta_2 c_2 H_2},$$
$$\bar{p} = \frac{\alpha_2}{H_2\beta_2 c_2}\left[\frac{\rho_2 c_2}{1+\rho_2 b_2 c_2} - d_2 - \delta_2\bar{n}_2\right]. \tag{9}$$

The model with $n_1 = 0$ is equivalent to the Rosenzweig-MacArthur model.

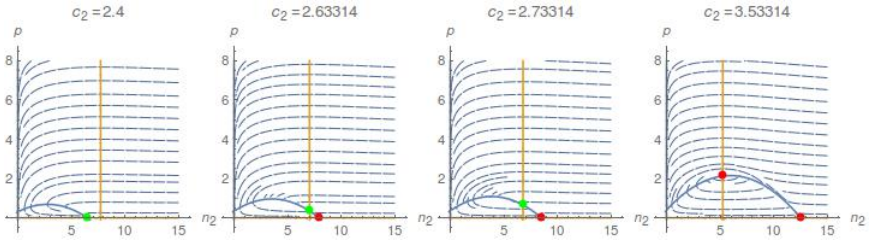

Figure 11: Dynamics in the (n_2, p)-plane. The blue parabola is the n_2-isocline and the orange line is the n_1-isocline. Green dots are stable equilibria and red dots are unstable ones.
$\delta_2 = 0.04, b_2 = 0.4, \rho_2 = 0.9, \beta_2 = 0.9, h_2 = 0.5, \epsilon = 0.5, \alpha_2 = 0.7$.

As before, $\bar{p}$ is positive when $c_2 > \tilde{c}_2$ and the n_2-isocline (the blue parabola) intersects the p-isocline (the orange line) in Fig.11. The main difference with the case $h_2 = 0$ is that the stability of $(\bar{n}_2, \bar{p})$ depends upon the value of c_2. When c_2 increases the p-isocline moves on the left. When the line reaches the maximum of the parabola a supercritical Hopf bifurcation occurs. This happens when c_2 is equal to

$$\bar{c}_2 = \frac{\beta_2 h_2 d_2 H_2 + \delta_2\rho_2 b_2\tilde{H}_2 + \sqrt{(\beta_2 h_2 d_2 H_2 + \delta_2\rho_2 b_2\tilde{H}_2)^2 + 4\delta_2\tilde{H}_2 H_2\beta_2 h_2 D_2\rho_2}}{2H_2\beta_2 h_2\rho_2 D_2}$$

with $\tilde{H}_2 = (1-q)\alpha_2 + h_2\epsilon$. For $c_2 > \bar{c}_2$, $(\bar{n}_2, \bar{p})$ is no longer stable and solutions converge to a stable limit cycle. Assuming $c_2 < \bar{c}_2$, transversal stability in the three-dimension space is still determined by the eigenvalue

$$\lambda_t = -d_1 + \frac{\rho_1 c_1}{1+\rho_1 b_1 c_1} - q\beta_1 c_1\bar{p}.$$

We can derive same conclusions as before: if $\bar{p} > \bar{p}_{y_1}$, λ_t is negative for every $c_1 > 0$, if $\bar{p} < \bar{p}_{y_1}$, λ_t is positive for $c_1^- < c_1 < c_1^+$. Note that formulas for $\bar{p}_{y_1}$ and $c_1^{\pm}$ still hold. What also still hold are the values for $\bar{n}_1^{\pm}$ and the results about their existence and stability. These results are summarized in Fig.12. The light blue region means no positive internal equilibria, i.e. $\bar{p} < \bar{p}_{crit} \wedge \lambda_t < 0 \wedge c_1 < \tilde{c}_1$ or $\bar{p} > \bar{p}_{crit}$, with

$$\bar{p}_{crit}(c_1) = \frac{\left[c_1\beta_1 h_1(B(c_1) - d_1) + \delta_1\right]^2}{4q\delta_1\beta_1^2 h_1 c_1^2}.$$

The red region marks where only $\bar{n}^+$ is positive, meaning $\bar{p} < \bar{p}_{crit}$ and $\lambda_t > 0$. In the purple area both $\bar{n}_1^{\pm}$ exits real and positive and $\lambda_t < 0 \wedge c_1 > \tilde{c}_1 \wedge \bar{p} < \bar{p}_{crit}$. $(\bar{n}_1^+, \bar{n}_2, \bar{p})$ is always stable when positive and $c_2 < \bar{c}_2$ and $(\bar{n}_1^-, \bar{n}_2, \bar{p})$ is always unstable when it is positive. Equilibria stability

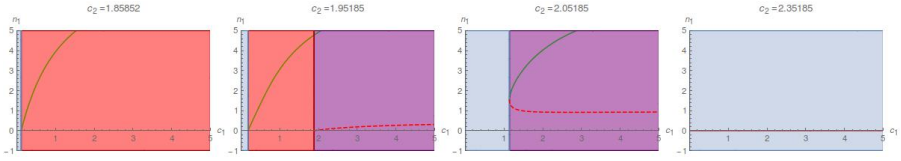

Figure 12: Regions of existence conditions for $\bar{n}_1^{\pm}$ for different values of c_2. Green line for $\bar{n}_1^+$, red and dashed line for $\bar{n}_1^-$. On the abscissa axis the stability of $(0, \bar{n}_2, \bar{p})$, green for stable, red and dashed for unstable. $d_1 = 0.1, \delta_1 = 0.1, b_1 = 1, q = 0.6, h_1 = 0.7, \rho_1 = 1, \beta_1 = 1, d_2 = 0.9, \delta_2 = 0.01, b_2 = 0.4, \rho_2 = 0.9, \beta_2 = 0.9, h_2 = 0.5, \epsilon = 0.5, \alpha_2 = 0.7$.

regions for different values of c_1 and c_2 are summarized in Fig.13. In the intersection between the stability region of $(0, \bar{n}_2, \bar{p})$ and $(\bar{n}_1^+, \bar{n}_2, \bar{p})$ the equilibrium $(\bar{n}_1^-, \bar{n}_2, \bar{p})$ exists positive. Note that fold bifurcation can happen either when c_1 decreases or when c_2 decreases. In the upper white part the system converge either to a boundary or to an internal limit cycle. By changing δ_1 we can observe different shapes of this region, which consequences will be discussed later.

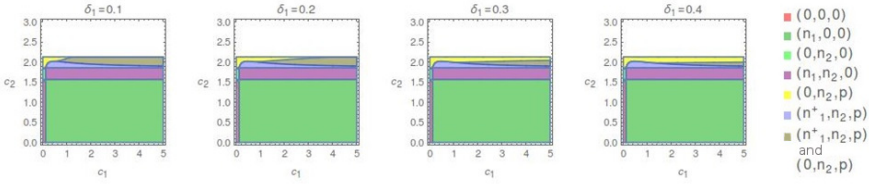

Figure 13: Equilibria stability regions as function of c_1 and c_2 for different values of δ_1. In the intersection between $(\bar{n}_1^+, \bar{n}_2, \bar{p})$ and $(0, \bar{n}_2, \bar{p})$ stability region, $\bar{n}_1^-$ is positive but the equilibrium is unstable. In the white region solutions converge either to a boundary or a internal limit cycle. $d_1 = 0.1, b_1 = 1, q = 0.6, h_1 = 1, \rho_1 = 1, \beta_1 = 1, d_2 = 0.9, \delta_2 = 0.01, b_2 = 0.4, \rho_2 = 0.9, \beta_2 = 0.9, h_2 = 0.5, \epsilon = 0.5, \alpha_2 = 0.7$.

Chosen c_1, one can observe in the numerical solutions, the changing behaviour due to c_2 increasing.

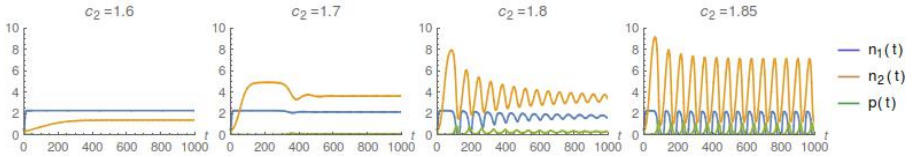

Figure 14: Numerical solutions of the model as function of time.
$c_1 = 2, d_1 = 0.1, \delta_1 = 0.25, b_1 = 1, q = 0.7, h_1 = 0.5, \rho_1 = 1, \beta_1 = 1, d_2 = 0.9, \delta_2 = 0.01, b_2 = 0.4, \rho_2 = 0.9, \beta_2 = 0.9, h_2 = 0.3, \epsilon = 0.5, \alpha_2 = 0.8.$

Same conclusions can be drawn from the phase plane of n_1 and p:

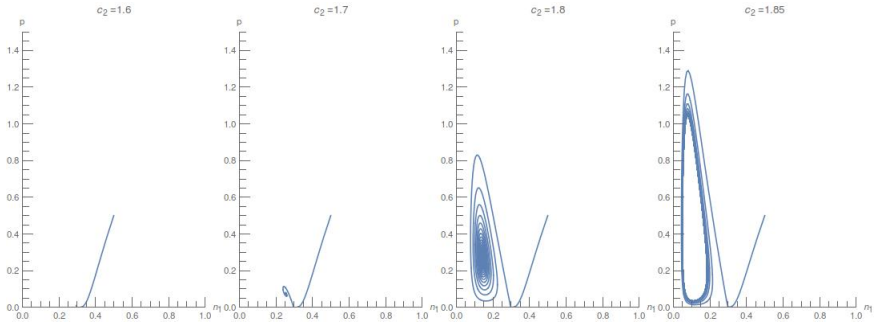

Figure 15: Numerical solutions of the model in the (n_1, p)-phase plane.
$c_1 = 0.21, d_1 = 0.1, \delta_1 = 0.25, b_1 = 1, q = 0.7, h_1 = 0.5, \rho_1 = 1, \beta_1 = 1, d_2 = 0.9, \delta_2 = 0.01, b_2 = 0.4, \rho_2 = 0.9, \beta_2 = 0.9, h_2 = 0.3, \epsilon = 0.5, \alpha_2 = 0.8.$

As stated before, the shape of the regions where $(\bar{n}_1^{\pm}, \bar{n}_2, \bar{p})$ are positive changes considerably with the changes in n_1 parameters. This shape is crucial to predict the behaviour of the system when periodical solutions appear. The main differences in the cycling behaviour are related to the values of c_2 at which the fold and the Hopf bifurcations occur. There are three possible cases. If the Hopf bifurcation happens for larger values of c_2 than the fold one, if it happens for smaller value and only $\bar{n}_1^+$ is positive, and if also $\bar{n}_1^-$ is positive. In the first case, the dynamics of $n_1^{\pm}$ is basically the same as in the case $h_2 = 0$. The shape of the equilibria stability region can be observed in the left pictures in Fig.16. When $c_2 < \tilde{c}_2$, we can apply Adaptive Dynamics theory starting on the positive and stable internal equilibrium $(\bar{n}_1^+, \bar{n}_2, \bar{p})$. Following similar steps as in $h_2 = 0$ case we can construct the selection gradient to obtain evolutionary suicide also in this case, as shown in the right panel of Fig.16. In the second case, the Hopf bifurcation occurs when only $\bar{n}^+$ is positive. In Fig.17 this happens when the horizontal line of the Hopf bifurcation crosses the light green region. An internal stable cycle generates from $(\bar{n}_1^+, \bar{n}_2, \bar{p})$ when $c_2 = \tilde{c}_2$. When $c_2 > \tilde{c}_2$, we can the define invasion fitness and selection gradients as

$$s_x(y) = \left(-d_1 + \frac{\rho_1 y}{1 + \rho_1 b_1 y}\right) - \delta_1 E_1(x) - q\beta_1 y E_2(x)$$
$$[\partial_y s_x(y)]_{y=x} = \frac{\rho_1}{(1 + b_1\rho_1 x)^2} - q\beta_1 E_2(x),$$

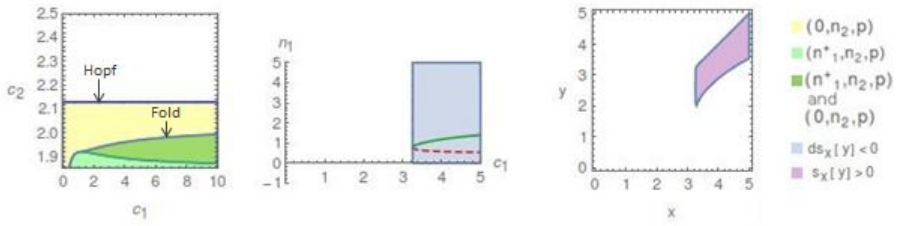

Figure 16: Evolutionary suicide in the case $h_2 \neq 0$. In the first panel, in the light green region $\bar{n}_1^+ > 0$ in the darker green one $\bar{n}_1^\pm > 0$, and in the yellow one $\bar{n}_1^\pm$ are complex. The Hopf bifurcation occurs on the blue line and in the upper white part solutions converge either to a boundary or an internal limit cycle. In the second pane, the selection gradient is negative in the light blue region . $d_1 = 0.3, \delta_1 = 0.25, b_1 = 1, q = 0.6, h_1 = 1, \rho_1 = 1, \beta_1 = 1, d_2 = 0.9, \delta_2 = 0.01, b_2 = 0.4, \rho_2 = 0.9, \beta_2 = 0.9, h_2 = 0.5, \epsilon = 0.5, \alpha_2 = 0.7$. In the second and third panel $c_2 = 1.95185$.

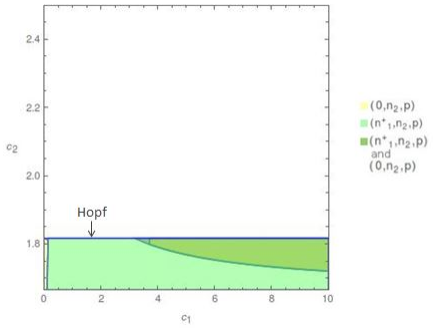

Figure 17: Existence and stability region of $\bar{n}^\pm$. Colour regions are the same as Fig.16. $d_1 = 0.1, \delta_1 = 0.25, b_1 = 1, q = 0.7, h_1 = 0.5, \rho_1 = 1, \beta_1 = 1, d_2 = 0.9, \delta_2 = 0.01, b_2 = 0.4, \rho_2 = 0.9, \beta_2 = 0.9, h_2 = 0.3, \epsilon = 0.5, \alpha_2 = 0.8$.

with T period length of the limit cycle, $(\bar{n}_1^+(t), \bar{p}(t))$ limit cycle trajectory and

$$E_1(x) = \frac{1}{T}\int_0^T \bar{n}_1^+(t)dt$$
$$E_2(x) = \frac{1}{T}\int_0^T \frac{\bar{p}(t)}{1 + h_1\beta_1 x\bar{n}_1^+(t)}dt.$$

The division by T preserves the dimension of a rate for $s_x(y)$. Note that

$$\left[\partial_y^2 s_x(y)\right]_{y=x} = -\frac{2b_1\rho_1^2}{(1+b_1\rho_1 x)^3} < 0, \quad \forall x > 0.$$

Thus, every convergence stable limit cycle is also evolutionary stable. An example of convergence stable of limit cycle is provided in Fig.18. In the left picture are shown the numerical solution

estimated by the package MatCont with a method of continuation of limit solution. In the right picture is plotted the numerical selection gradient integrated over the interpolated solutions using the trapezoidal rule.

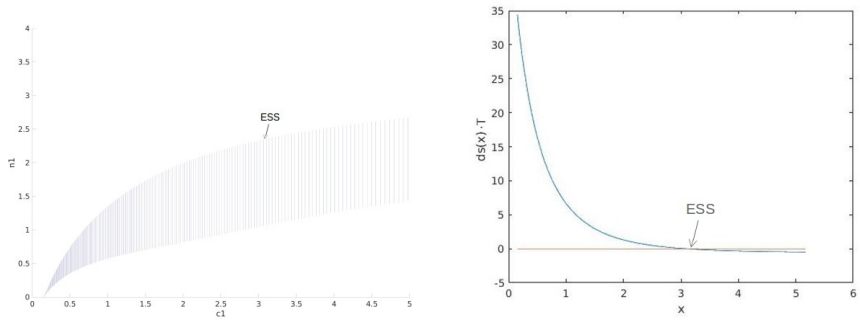

Figure 18: Evolution toward an ESS. $d_1 = 0.1, \delta_1 = 0.25, b_1 = 1, q = 0.7, h_1 = 0.5, \rho_1 = 1, \beta_1 = 1, c_2 = 1.8216172, d_2 = 0.9, \delta_2 = 0.01, b_2 = 0.4, \rho_2 = 0.9, \beta_2 = 0.9, h_2 = 0.3, \epsilon = 0.5, \alpha_2 = 0.8$.

The most interesting case is when the Hopf bifurcation occurs before the fold one while both $\bar{n}_1^+$ and $\bar{n}_1^-$ are positive, like in the first two panels in Fig.13, in Fig.19 and in the right half of Fig.17.

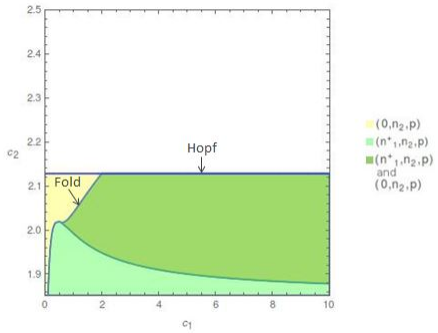

Figure 19: Existence and stability region of $\bar{n}^{\pm}$. Colour regions are the same as Fig.16. $d_1 = 0.1, \delta_1 = 0.1, b_1 = 1, q = 0.6, h_1 = 0.7, \rho_1 = 1, \beta_1 = 1, d_2 = 0.9, \delta_2 = 0.01, b_2 = 0.4, \rho_2 = 0.9, \beta_2 = 0.9, h_2 = 0.5, \epsilon = 0.5, \alpha_2 = 0.7$.

A stable cycle generates from $(\bar{n}_1^+, \bar{n}_2, \bar{p})$ and an unstable one generates from $(\bar{n}_1^-, \bar{n}_2, \bar{p})$. Moreover, chosen $c_2 > \bar{c}_2$ and let c_1 decrease a fold bifurcation happens between the two cycles. It is possible to observe this behaviour by plotting the Poincaré maps for different values of c_1 as in Fig.20. Unfortunately, we can only use values for c_2 close to $\bar{c}_2$. For larger values of c_2, the system becomes too stiff and the numerical simulation fails. In particular, n_1 starts assuming negative values while the system is positive preserving. Anyway, it is possible to construct an example of evolutionary suicide over the cycle fold bifurcation for c_2 slightly larger than $\bar{c}_2$. The idea is to start from initial values for c_1 and c_2 such that both $\bar{n}_1^{\pm}$ are biologically feasible but $c_2 < \bar{c}_2$. Then, we use MatCont to continue the equilibrium $(\bar{n}_1^+, \bar{n}_2, \bar{p})$ when c_2 changes and plot both branches

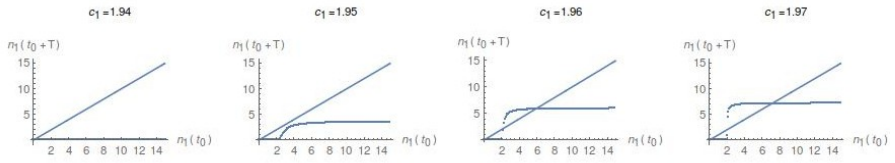

Figure 20: Poincaré maps for the cycle fold bifurcation.
$d_1 = 0.3, \delta_1 = 0.03, b_1 = 1, q = 0.6, h_1 = 1, \rho_1 = 1, \beta_1 = 1, c_2 = 3.45629, d_2 = 0.9, \delta_2 = 0.04, b_2 = 0.4, \rho_2 = 0.9, \beta_2 = 0.9, h_2 = 0.5, \epsilon = 0.5, \alpha_2 = 0.7, t_0 = 1054.24, \mathrm{T} = 69.7309.$

of the equilibrium fold bifurcation. In Fig.21 we can note the two Hopf bifurcation points (H) and the fold bifurcation point (LP). MatCont can also plot the limit cycle that generates from an Hopf bifurcation point. Continuations of the two limit cycles for c_2 increasing can be seen on the right of the points marked with H. MatCont numerically computes the multipliers of the cycles, i.e. the eigenvalues of the Poincaré map at the cycles. As stated, the upper cycles have all multipliers with modulus less than one and are therefore stable. The cycles started from the lower branch of equilibria have a multiplier with modulus bigger than one and is unstable. The selection gradient has been constructed to be still negative at the Hopf bifurcation point by choosing $h_1 = 0.7$. In Fig.21, the point SG marks where the selection gradient becomes equal to zero. It is positive for smaller value of c_2 and negative for larger,in particular for $c_2 = \bar{c}_2$. Thus, for continuity, the selection gradient is going to be negative for small cycles. Then, we fix the value of c_2 slightly larger

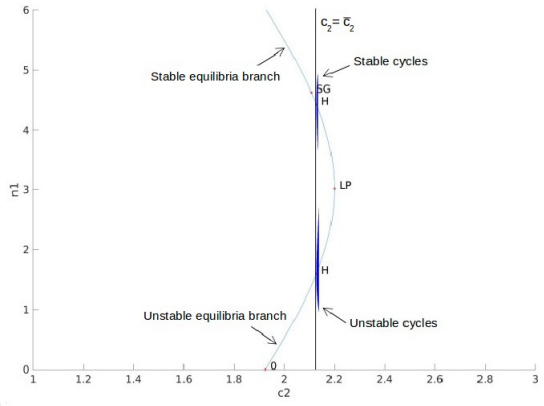

Figure 21: Equilibria fold bifurcation when c_2 varies. H=Hopf bifurcation, LP=saddle-node bifurcation, SG=selection gradient equal to zero. $d_1 = 0.1, \delta_1 = 0.1, c_1 = 3, b_1 = 1, q = 0.6, h_1 = 0.7, \rho_1 = 1, \beta_1 = 1, d_2 = 0.9, \delta_2 = 0.01, b_2 = 0.4, \rho_2 = 0.9, \beta_2 = 0.9, h_2 = 0.5, \epsilon = 0.5, \alpha_2 = 0.7.$

then $\bar{c}_2$ and compute the stable limit cycle for this parameters choice. In Fig.21 it is the right most cycle branching from the upper branch. We can now continue it when c_1 decreases and observe the consequent cycle bifurcation curve in Fig.22. For smaller value of c_1 than the bifurcation value solutions converge to the boundary limit cycle in (n_2, p)-plane. Numerical integration of the selection gradient confirms that it is negative on the cycle fold bifurcation point (Fig.23). Thus, this is an

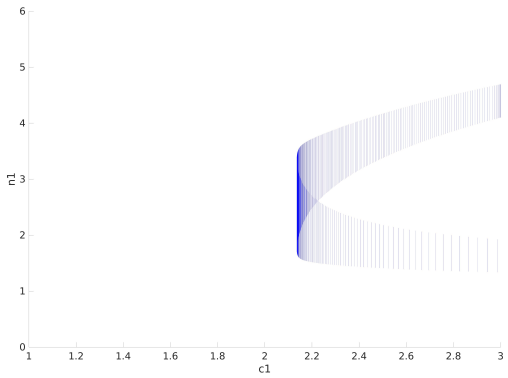

Figure 22: Cycle fold bifurcation when c_1 varies. $d_1 = 0.1, \delta_1 = 0.1, b_1 = 1, q = 0.6, h_1 = 0.7, \rho_1 = 1, \beta_1 = 1, d_2 = 0.9, \delta_2 = 0.01, b_2 = 0.4, c_2 = 2.1296215, \rho_2 = 0.9, \beta_2 = 0.9, h_2 = 0.5, \epsilon = 0.5, \alpha_2 = 0.7$.

example of evolutionary suicide on limit cycles.

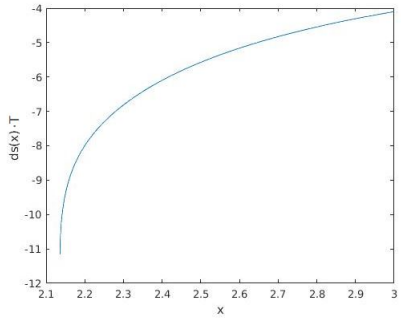

Figure 23: Numerical integration of the selection gradient over cycles.
$d_1 = 0.1, \delta_1 = 0.1, b_1 = 1, q = 0.6, h_1 = 0.7, \rho_1 = 1, \beta_1 = 1, d_2 = 0.9, \delta_2 = 0.01, b_2 = 0.4, \rho_2 = 0.9, \beta_2 = 0.9, c_2 = 2.1296215, h_2 = 0.5, \epsilon = 0.5, \alpha_2 = 0.7$.

2.3 Critical function analysis

The idea is to generalize the model by assuming that the relation between birth rate and feeding effort of the first prey species is expressed by a not-specified function $B(c_1)$. Under which conditions is it still possible to have evolutionary suicide? It is possible to construct $B(c_1)$ such that the

evolutionary suicide occurs? The model becomes

$$\begin{aligned}
\frac{dn_1}{dt} &= \left(-d_1 - \delta_1 n_1 + B(c_1) - \frac{q\beta_1 c_1 p}{1 + h_1 c_1 \beta_1 n_1}\right) n_1 \\
\frac{dn_2}{dt} &= \left(-d_2 - \delta_2 n_2 + \frac{\rho_2 c_2}{1 + \rho_2 b_2 c_2} - \frac{(1-q)\beta_2 c_2 p}{1 + h_2 \beta_2 c_2 n_2}\right) n_2 \\
\frac{dp}{dt} &= \left(-\epsilon + \frac{\alpha_2 (1-q)\beta_2 c_2 n_2}{1 + h_2 \beta_2 c_2 n_2}\right) p.
\end{aligned}$$

Since $\alpha_1 = 0$, the system is still decoupled such that the dynamics of (n_2, p) is independent of n_1. Equilibrium values and stability of $(0, \bar{n}_2, \bar{p})$ in the (n_2, p)-plane are not affected by the choice of $B(c_1)$. From now on we assume that the equilibrium $(\bar{n}_2, \bar{p})$ is stable in the (n_2, p)-plane. What changes from the dynamics discussed before is the eigenvalue that determines the transversal stability of $(0, \bar{n}_2, \bar{p})$,

$$\lambda_t = B(c_1) - d_1 - q\beta_1 c_1 \bar{p}.$$

When $\bar{p} > \tilde{p}(c_1) = (B(c_1) - d_1)/q\beta_1 c_1$, $\lambda_t < 0$ and $(0, \bar{n}_2, \bar{p})$ is locally stable. The internal equilibria are, as before,

$$\begin{aligned}
\bar{n}_1^{\pm} &= \frac{c_1\beta_1 h_1 (B(c_1) - d_1) - \delta_1 \pm \sqrt{\Delta}}{2\delta_1 c_1 \beta_1 h_1}, \\
\text{with } \Delta &= \left(c_1\beta_1 h_1 (B(c_1) - d_1) - \delta_1\right)^2 + 4\delta_1 c_1 \beta_1 h_1 (B_1(c_1) - d_1 - q\beta_1 c_1 \bar{p}).
\end{aligned}$$

Again, in order to have both $\bar{n}_1^+$ and $\bar{n}_1^-$ positive the following conditions must satisfied

$$\begin{aligned}
B(c_1) - d_1 - q\beta_1 c_1 \bar{p} &< 0, \\
c_1\beta_1 h_1 (B(c_1) - d_1) - \delta_1 &> 0, \\
\Delta &> 0.
\end{aligned}$$

They can be rewritten as

$$\tilde{p}(c_1) < \bar{p} < \bar{p}_{crit}(c_1), \tag{10a}$$

$$B(c_1) > d_1 + \frac{\delta_1}{h_1 c_1 \beta_1}, \tag{10b}$$

with

$$\bar{p}_{crit}(c_1) = \frac{\left[c_1\beta_1 h_1 (B(c_1) - d_1) + \delta_1\right]^2}{4q\delta_1 \beta_1^2 h_1 c_1^2}.$$

Note that $\tilde{p}(c_1) \leq \bar{p}_{crit}(c_1)$, since

$$\begin{aligned}
\frac{B_1(c_1) - d_1}{q\beta_1 c_1} &\overset{?}{\leq} \frac{\left[c_1\beta_1 h_1 (B(c_1) - d_1) + \delta_1\right]^2}{4q\delta_1 \beta_1^2 h_1 c_1^2} \\
(4\delta_1\beta_1 h_1 c_1)(B_1(c_1) - d_1) &\overset{?}{\leq} \left[c_1\beta_1 h_1 (B(c_1) - d_1) + \delta_1\right]^2 \\
0 &\leq \left[c_1\beta_1 h_1 (B(c_1) - d_1) - \delta_1\right]^2.
\end{aligned}$$

Under the assumption that $c_2 < \bar{c}_2$, meaning that in the (n_2, p)-plane the Hopf bifurcation has not occurred, the local stability of $\bar{n}_1^{\pm}$ is not affected by $B(c_1)$, as long they are positive. To prove this, we look at the sign of the eigenvalues of the Jacobian matrix evaluated at the two equilibria

$$J = \begin{pmatrix} -\delta\bar{n}_1 + \frac{q\beta_1^2 c_1^2 h_1 \bar{p}\bar{n}_1}{(1+c_1\beta_1 h_1 \bar{n}_1)^2} & 0 & -\frac{q\beta_1 c_1 \bar{n}_1}{1+h_1 c_1 \beta_1 \bar{n}_1} \\ 0 & \frac{\rho_2 c_2}{1+b_2\rho_2 c_2} - d_2 - (1-q)\beta_2 c_2 \bar{p} & -\frac{\epsilon}{\alpha_2} \\ 0 & H_2\beta_2 c_2 \bar{p} & 0 \end{pmatrix}.$$

The eigenvalues are

$$\lambda_1(\bar{n}_1) = -\delta\bar{n}_1 + \frac{q\beta_1^2 c_1^2 h_1 \bar{p}\bar{n}_1}{(1+c_1\beta_1 h_1 \bar{n}_1)^2}$$

and the two eigenvalues of

$$J_{(n_2,p)} = \begin{pmatrix} \frac{\rho_2 c_2}{1+b_2\rho_2 c_2} - d_2 - (1-q)\beta_2 c_2 \bar{p} & -\frac{\epsilon}{\alpha_2} \\ H_2\beta_2 c_2 \bar{p} & 0 \end{pmatrix}. \tag{11}$$

The eigenvalues of $J_{(n_2,p)}$ correspond to the ones of $(0, \bar{n}_2, \bar{p})$ in the (n_2, p)-plane, they are independent of c_1 and have negative real part since $c_2 < \bar{c}_2$. Thus, the stability of $n_1^{\pm}$ is determined by $\lambda_1(\bar{n}_1)$. After evaluating $\lambda_1(\bar{n}_1)$ at $\bar{n}_1^+$, further simplification yields

$$\lambda_1(\bar{n}_1^+) = -\frac{\sqrt{\Delta}}{2\delta_1(1+c_1\beta_1 h_1 \bar{n}_1^+)} < 0.$$

Note that Δ is positive under condition (10a). When we evaluate $\lambda_1(\bar{n}_1)$ at $\bar{n}_1^-$ we get

$$\lambda(\bar{n}_1^-) = \frac{\sqrt{\Delta}}{2\delta_1(1+c_1\beta_1 h_1 \bar{n}_1^-)} > 0.$$

The fold bifurcation occurs at

$$\bar{n}_{crit}(c_1) = \frac{c_1\beta_1 h_1(B(c_1) - d_1) - \delta_1}{2\delta_1 c_1 \beta_1 h_1},$$

when $\Delta = 0$. This condition is satisfied when

$$\bar{p} = \bar{p}_{crit}(c_1). \tag{12}$$

To construct the function $B(c_1)$, we start by choosing a value $c_1^* > 0$ where we want the fold bifurcation to happen. We pick a value $B^* > 0$, with $B^* = B(c_1^*)$ such that the condition (10b) evaluated at c_1^* is satisfied and we compute the value of $\bar{p}_{crit}(c_1^*)$. Then, we need to find the parameter set for n_2 and p such that $\bar{p}$ solves $\bar{p} = \bar{p}_{crit}(c_1^*)$ with $c_2 < \bar{c}_2$. Remind from (9) that

$$\bar{p} = \frac{\alpha_2}{((1-q)\alpha_2 - h_2\epsilon)\beta_2 c_2}\left[\frac{\rho_2 c_2}{1+\rho_2 b_2 c_2} - d_2 - \frac{\delta_2\epsilon}{\beta_2 c_2((1-q)\alpha_2 - h_2\epsilon)}\right].$$

We now show that it is always possible to chose the parameter set for n_2 such that (12) is satisfied at c_1^*. We start from a parameter set that gives a predator equilibrium value $\hat{p}$ such that $\hat{p} \neq \bar{p}_{crit}(c_1^*)$ and $(\bar{n}, \hat{p})$ is stable in the (n_2, p)-plane. We define $\gamma = \bar{p}_{crit}(c_1^*)/\hat{p}$ and we construct a new parameter

set that gives as predator equilibrium $\bar{p}^* = \gamma\hat{p}$. Precisely, we multiply ρ_2 and d_2 by γ and divide b_2 by γ. Moreover, we prove that the stability in the (n_2, p)-plane is preserved. Indeed, we define $J_{(\bar{n}_2,\hat{p})}$ as the Jacobian matrix (11) evaluated at $(\bar{n}_2, \hat{p})$, and $J_{(\bar{n}_2,\bar{p}^*)}$ as the Jacobian matrix evaluated at $(\bar{n}_2, \bar{p}^*)$ with the new parameter set. We use the trace-determinant criteria to check that the eigenvalues of $J_{(\bar{n}_2,\bar{p}^*)}$ have negative real part. Note that

$$\begin{aligned}\det(J_{(\bar{n}_2,\bar{p}^*)}) &= \det(J_{(\bar{n}_2,\hat{p})}) > 0\\ \operatorname{tr}(J_{(\bar{n}_2,\bar{p}^*)}) &= \gamma \operatorname{tr}(J_{(\bar{n}_2,\hat{p})}) < 0,\end{aligned}$$

since $(\bar{n}_2, \hat{p})$ is stable in the (n_2, p)-plane by assumption. We conclude that $(\bar{n}_2, \bar{p}^*)$ is stable in the (n_2, p)-plane and satisfies (12).

Thus, for every function $B(c_1)$ that intersects the point (c_1^*, B^*) the model will show a fold bifurcation at c_1^*. The question now is how to get evolutionary suicide. Note that, if the two branches of equilibria of the fold bifurcation open to the right we would need a negative selection gradient at the fold bifurcation. Likewise, if the two branches of equilibria of the fold bifurcation open to the left we would need a positive selection gradient at the fold bifurcation. We prove now that the second case is impossible. We cannot have a positive selection gradient at the bifurcation point when the fold bifurcation opens to the left. The two branches of the fold bifurcation open to the left when $p_{crit}(c_1) > \bar{p}$ (condition (10a)) for values of c_1 smaller than c_1^*. This happens if

$$\begin{aligned} p'_{crit}(c_1^*) &< 0\\ &\Updownarrow\\ c_1\beta_1 h_1^*(B'(c_1^*)c_1^* + B^* - d_1) - c_1^*\beta_1 h_1(B^* - d_1) - \delta_1 &< 0\\ &\Updownarrow\\ B'(c_1^*) &< \frac{\delta_1}{(c_1^*)^2\beta_1 h_1}. \end{aligned} \tag{13}$$

Then, we define as before

$$g(c_1^*) = B'(c_1^*) - \frac{q\beta_1\bar{p}_{crit}(c_1^*)}{1 + h_1\beta_1 c_1^*\bar{n}_{crit}(c_1^*)},$$

as the selection gradient evaluated at $(\bar{n}_{crit}, \bar{p}_{crit})$. The condition for positive $g(c_1^*)$ is that

$$B'(c_1^*) > \frac{1}{2c_1^*}\left(B^* - d_1 + \frac{\delta_1}{\beta_1 c_1^* h_1}\right). \tag{14}$$

We finish the proof by showing that (13) and (14) can not hold at the same time because the right hand side of (13) is always smaller than the right hand side of (14) when (10b) is satisfied:

$$\begin{aligned} \frac{\delta_1}{(c_1^*)^2\beta_1 h_1} &\overset{?}{<} \frac{1}{2c_1^*}\left(B^* - d_1 + \frac{\delta_1}{\beta_1 c_1^* h_1}\right)\\ \frac{2\delta_1}{c_1^*\beta_1 h_1} &\overset{?}{<} B_1^* - d_1 + \frac{\delta_1}{c_1^*\beta_1 h_1}\\ \frac{\delta_1}{c_1^*\beta_1 h_1} &\overset{?}{<} B_1^* - d_1\\ 0 &< c_1^*\beta_1 h_1(B_1^* - d_1) - \delta_1 \end{aligned}$$

where the last inequality holds for condition (10b). Thus, we proved that in this model evolutionary suicide can not occur when the fold bifurcation opens to the left. The only case possible is that the evolutionary suicide happens on the fold bifurcation when it opens to the right. In fact, to have a fold bifurcation that opens on the right we need $p'_{crit}(c_1*) > 0$, i.e.

$$B'(c_1^*) > \frac{\delta_1}{(c_1^*)^2\beta_1 h_1},$$

to have a negative selection gradient on the fold bifurcation we need

$$B'(c_1^*) < \frac{1}{2c_1^*}\left(B^* - d_1 + \frac{\delta_1}{\beta_1 c_1^* h_1}\right),$$

and we have already proven that at the bifurcation point

$$\frac{\delta_1}{(c_1^*)^2\beta_1 h_1} < \frac{1}{2c_1^*}\left(B^* - d_1 + \frac{\delta_1}{\beta_1 c_1^* h_1}\right).$$

Thus, to have evolutionary suicide we only have to choose the slope of $B(c_1)$ at (c_1^*, B_1^*) such that

$$\frac{\delta_1}{(c_1^*)^2\beta_1 h_1} < B'(c_1^*) < \frac{1}{2c_1^*}\left(B^* - d_1 + \frac{\delta_1}{\beta_1 c_1^* h_1}\right). \tag{15}$$

To summarize, we have shown that, with an appropriate choice of the parameter set for the second-type species, using a generic function $B(c_1)$ that crosses (c_1^*, B^*) with a slope that satisfy (15) the evolutionary suicide will occur.

We show now an example of this. First we fix the values of c_1^*, B^*, B_s^*, the slope at c_1^*, and the parameter set for the second-type prey according to the conditions analysed before. Then, we choose a family of function, for example

$$B(c_1) = a c_1^{r_1}(1 + f c_1)^{r_2}.$$

and determine a and f by solving

$$B(c_1^*) = B^*$$
$$B'(c_1^*) = B_s^*.$$

Then, by plotting $\bar{p}$, $\tilde{p}(c_1)$, and $\bar{p}_{crit}(c_1)$, we check conditions (10) for different choices of r_1 and r_2.

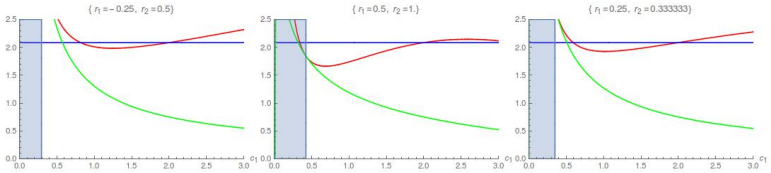

Figure 24: Conditions (10). The red curve is $\bar{p}_{crit}(c_1)$,the green is $\tilde{p}(c_1)$ and the blue line represents $\bar{p}$. The light blue region marks when condition (10b) does not apply.
$c_1^* = 2, B^* = 1, B_s^* = 0.1, d_1 = 0.1, \delta_1 = 0.1, q = 0.6, h_1 = 0.5, \beta_1 = 1, c_2 = 2.45409, d_2 = 0.9, \delta_2 = 0.01, b_2 = 0.4, \rho_2 = 0.9, \beta_2 = 0.9, h_2 = 0.5, \epsilon = 0.5, \alpha_2 = 0.7.$

As expected, (10) are satisfied at c_1^*. Thus, in the three cases the system shows a fold bifurcation in c_1^*. Then, we check condition (15) by plotting $B'(c_1)$ and the two boundary terms of (15).

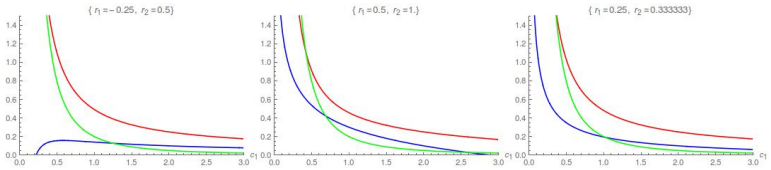

Figure 25: Condition (15).The red line represents the right term of (15), the green one represents the left term of (15) and the blue one is $B'(c_1)$. $c_1^* = 2, B^* = 1, c_2^* = 2.45409, B_s^* = 0.1, d_1 = 0.1, \delta_1 = 0.1, q = 0.6, h_1 = 0.5, \beta_1 = 1, d_2 = 0.9, \delta_2 = 0.01, b_2 = 0.4, \rho_2 = 0.9, \beta_2 = 0.9, h_2 = 0.5, \epsilon = 0.5, \alpha_2 = 0.7, c_1 = 2$.

As claimed, the three functions satisfy the condition in a neighbourhood of the bifurcation point. To confirm the presence of evolutionary suicide we plot $\bar{n}_1^{\pm}$ as function of c_1 and the region where the selection gradient is negative in Fig.26.

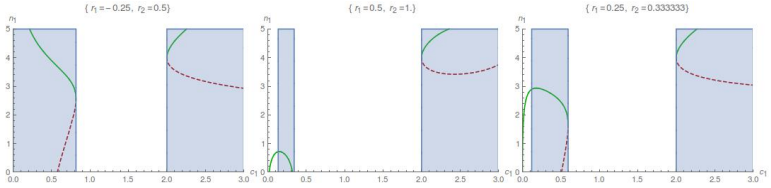

Figure 26: $\bar{n}_1^{\pm}$ as function of c_1 for different $B(c_1)$. Green line for $\bar{n}_1^{+}$, red and dashed line for $\bar{n}_1^{-}$. Where $\bar{n}_1^{+}$ is real and positive, the selection gradient is negative in the blue region and positive in the white one. $c_1^* = 2, B^* = 1, c_2^* = 2.45409, B_s^* = 0.1, d_1 = 0.1, \delta_1 = 0.1, q = 0.6, h_1 = 0.5, \beta_1 = 1, d_2 = 0.9, \delta_2 = 0.01, b_2 = 0.4, \rho_2 = 0.9, \beta_2 = 0.9, h_2 = 0.5, \epsilon = 0.5, \alpha_2 = 0.7, c_1 = 2$

3 The full model ($\alpha_1 \neq 0$))

As stated before, the full system is

$$\begin{aligned}
\frac{dn_1}{dt} &= \left(-d_1 - \delta_1 n_1 + \frac{\rho_1 c_1}{1+\rho_1 b_1 c_1} - \frac{q\beta_1 c_1 p}{1+h_1 c_1 \beta_1 n_1}\right) n_1 \\
\frac{dn_2}{dt} &= \left(-d_2 - \delta_2 n_2 + \frac{\rho_2 c_2}{1+\rho_2 b_2 c_2} - \frac{(1-q)\beta_2 c_2 p}{1+h_2 c_2 \beta_2 n_2}\right) n_2 \\
\frac{dp}{dt} &= \left(-\epsilon + \frac{\alpha_1 q \beta_1 c_1 n_1}{1+h_1\beta_1 c_1 n_1} + \frac{\alpha_2(1-q)\beta_2 c_2 n_2}{1+h_2\beta_2 c_2 n_2}\right) p.
\end{aligned}$$

The stability of trivial equilibria is summarized in the following table

Equilibrium	Positivity	Stability
$(0,0,0)$		$c_1 < c_1^0 \wedge c_2 < c_2^0$
$(n_1^0, 0, 0)$	$c_1 > c_1^0$	$c_2 < c_2^0 \wedge c_1 < \tilde{c}_1^+$
$(0, n_2^0, 0)$	$c_2 > c_2^0$	$c_1 < c_1^0 \wedge c_2 < \tilde{c}_2^+$
$(n_1^0, n_2^0, 0)$	$c_1 > c_1^0 \wedge c_2 > c_2^0$	$\varphi(c_1, c_2) < 0$

where

$$\begin{aligned}
n_i^0 =& \frac{1}{\delta_i}\left(\frac{\rho_i c_i}{1+\rho_i b_i c_i} - d_i\right) \\
c_i^0 =& \frac{d_i}{\rho_i(1-b_i d_i)} \\
\tilde{c}_i^{\pm} =& \frac{\epsilon\delta_i b_i \rho_i + d_i H_i \beta_i \pm \sqrt{(\epsilon\delta_i b_i\rho_i + d_i H_i\beta_i)^2 + 4\epsilon\delta_i H_i \rho_i \beta_i D_i}}{2H_i\rho_i\beta_i D_i} \\
D_i =& 1 - b_i d_i, \text{ with } i = 1,2 \\
H_1 =& \alpha_1 q - h_1 \epsilon \\
H_2 =& \alpha_2(1-q) - h_2\epsilon \\
\phi(c_1,c_2) =& -\epsilon + \frac{\alpha_1 q\beta_1 c_1(\rho_1 c_1 D_1 - d_1)}{\delta_1(1+\rho_1 b_1 c_1) + h_1\beta_1 c_1(\rho_1 c_1 D_1 - d_1)} \\
&+ \frac{\alpha_2(1-q)\beta_2 c_2(\rho_2 c_2 D_2 - d_2)}{\delta_2(1+\rho_2 b_2 c_2) + h_2\beta_2 c_2(\rho_2 c_2 D_2 - d_2)}.
\end{aligned}$$

By assumption, D_i, for $i = 1, 2$, and H_2 are positive. Since we are interested in the behaviour for small α_1 we consider the case when H_1 is negative. If $-\epsilon\delta_1 b_1 \rho_1 d_1 \beta_1 < H_1 < 0$, $(\bar{n}_1, 0, 0)$ is stable for every c_1. If $H_1 < -\epsilon\delta_1 b_1 \rho_1 d_1 \beta_1$, $(\bar{n}_1, 0, 0)$ is stable for $c_1 < \tilde{c}_1^- \vee c_1 < \tilde{c}_1^+$.

The equilibria $(\bar{n}_1, 0, \bar{p}_1)$ and $(0, \bar{n}_2, \bar{p}_2)$, with

$$\begin{aligned}
\bar{n}_i &= \frac{\epsilon}{H_i \beta_i c_i},\ i = 1, 2 \\
\bar{p}_1 &= \frac{1 + h_1 c_1 \beta_1 \bar{n}_1}{q \beta_1 c_1} \left(\frac{\rho_1 c_1}{1 + \rho_1 b_1 c_1} - d_1 - \delta_1 \bar{n}_1 \right) \\
\bar{p}_2 &= \frac{1 + h_2 c_2 \beta_2 \bar{n}_2}{(1-q) \beta_2 c_2} \left(\frac{\rho_2 c_2}{1 + \rho_2 b_2 c_2} - d_2 - \delta_2 \bar{n}_2 \right),
\end{aligned}$$

are positive respectively when $c_1 > \tilde{c}_1 \wedge H_1 > 0$ and $c_2 > \tilde{c}_2$. As before, $(\bar{n}_1, 0, \bar{p})$ loses stability in the (n_1, p)-plane for a supercritical Hopf bifurcation when $c_1 > \bar{c}_1$ and is transcritically stable $\forall c_2 > 0$ if $\bar{p} > \bar{p}_{y_1}$ and for $c_2 < c_2^+ \vee c_2 > c_2^-$ if $\bar{p} < \bar{p}_{y_2}$. Analogously, $(0, \bar{n}_2, \bar{p})$ loses stability in the (n_2, p)-plane for a supercritical Hopf bifurcation when $c_2 > \bar{c}_2$ and is transcritically stable $\forall c_1 > 0$ if $\bar{p} > \bar{p}_{y_2}$ and for $c_1 < c_1^+ \vee c_1 > c_1^-$ if $\bar{p} < \bar{p}_{y_2}$.

$$\begin{aligned}
\bar{c}_i &= \frac{d_i h_i H_i \beta_i + \tilde{H}_i \delta_i \rho_i b_i + \sqrt{(d_i h_i H_i \beta_i + \tilde{H}_i \delta_i \rho_i b_i)^2 + d_i \tilde{H}_i \delta_i H_i \rho_i h_i \beta_i D_i}}{2 H_i \rho_i h_i \beta_i D_i} \\
\tilde{H}_1 &= \alpha_1 q + h_1 \epsilon \quad \tilde{H}_2 = \alpha_2 (1-q) + h_2 \epsilon \\
\bar{p}_{y_1} &= \frac{\rho_2}{(1-q)\beta_2} (1 \pm \sqrt{d_2 b_2})^2 \quad \bar{p}_{y_2} = \frac{\rho_1}{q \beta_1} (1 \pm \sqrt{d_1 b_1})^2 \\
c_1^{\pm} &= \frac{\rho_1 D_1 - q \beta_1 \bar{p}_2 \pm \sqrt{(\rho_1 D_1 - q \beta_1 \bar{p}_2)^2 - 4 q d_1 \rho_1 \beta_1 b_1 \bar{p}_2}}{2 q \rho_1 \beta_1 b_1 \bar{p}_2} \\
c_2^{\pm} &= \frac{\rho_2 D_2 - (1-q) \beta_2 \bar{p}_1 \pm \sqrt{(\rho_2 D_2 - (1-q) \beta_2 \bar{p}_1)^2 - 4 (1-q) d_2 \rho_2 \beta_2 b_2 \bar{p}_1}}{2 (1-q) \rho_2 \beta_2 b_2 \bar{p}_1}
\end{aligned}$$

Stability regions of these equilibria are summarized in the next picture.

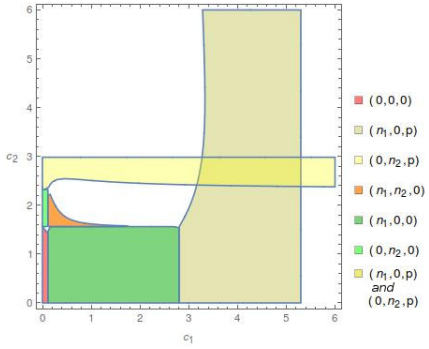

Figure 27: Stability regions of internal equilibria. $d_1 = 0.3, \delta_1 = 0.045, b_1 = 1, q = 0.6, \alpha_1 = 0.7, h_1 = 1, \rho_1 = 1, \beta_1 = 1, d_2 = 0.9, \delta_2 = 0.04, b_2 = 0.4, \rho_2 = 0.9, \beta_2 = 0.9, h_2 = 0.5, \epsilon = 0.5, \alpha_2 = 0.7$.

3.1 Numerical analysis of internal equilibria

Internal equilibria are solutions of the system

$$\begin{aligned} d_1 - \delta_1 n_1 + \frac{\rho_1 c_1}{1+\rho_1 b_1 c_1} - \frac{q\beta_1 c_1 p}{1+h_1 c_1 \beta_1 n_1} &= 0 \\ -d_2 - \delta_2 n_2 + \frac{\rho_2 c_2}{1+\rho_2 b_2 c_2} - \frac{(1-q)\beta_2 c_2 p}{1+h_2 c_2 \beta_2 n_2} &= 0 \\ -\epsilon + \frac{\alpha_1 q \beta_1 c_1 n_1}{1+h_1 \beta_1 c_1 n_1} + \frac{\alpha_2 (1-q)\beta_2 c_2 n_2}{1+h_2 \beta_2 c_2 n_2} &= 0 \end{aligned} \tag{16}$$

To find the solutions of (16) we have to solve a quartic form. Thus, the direct research of an explicit solution is both analytically and computationally difficult. The first approach that we choose to overcome the problem is to evaluate the system in every point of a grid in the (c_1, c_2)-plane and to solve it point-wise. In this way we can numerically evaluate the regions of (c_1-c_2) plane where internal equilibria are present as shown in Fig.28.

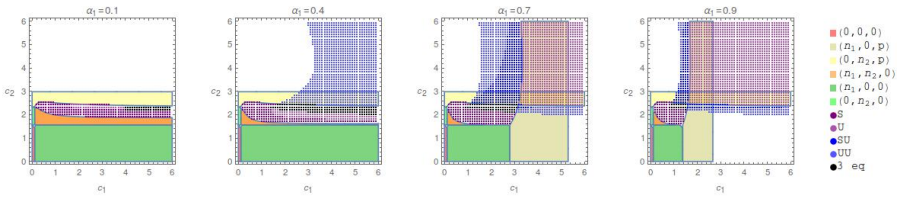

Figure 28: Regions of existence for the internal equilibria. $d_1 = 0.1, \delta_1 = 0.25, b_1 = 1, q = 0.6, h_1 = 0.7, \rho_1 = 1, \beta_1 = 1, d_2 = 0.9, \delta_2 = 0.03, b_2 = 0.4, \rho_2 = 0.9, \beta_2 = 0.9, h_2 = 0.5, \epsilon = 0.5, \alpha_2 = 0.7$.

To better understand transitions between different regions we can observe cross-sections of the plane. For example, we can see that a fold bifurcation happens when $\alpha_1 = 0.7$ and the system passes from a region with three equilibria (black one) to one with only a stable one (purple one) while c_1 decreases. In the case showed in Fig.29 the selection gradient is positive on the upper stable branch. Moreover the value of n_2 decreases while c_1 increases, since also the predator density increases. We can observe from the third panel of 28 that when we fix $c_2 = 2.352$, and move out from the black dots region by increasing c_1 we enter in the region where $(\bar{n}_1, 0, \bar{p})$ is stable. Thus, evolution does not lead to self-extinction of the first species but to the extinction of the second-type prey population through a transcritical bifurcation.

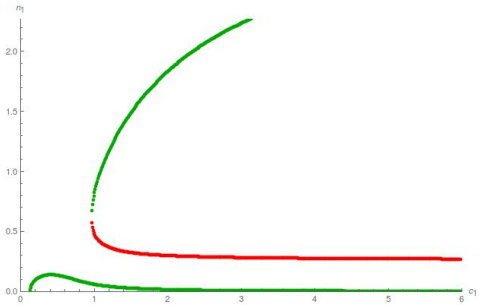

Figure 29: Cross-section for $c_2 = 2.352$ when $\alpha_1 = 0.7$. Green dots are for stable equilibria, red ones for unstable equilibria. $d_1 = 0.1, \delta_1 = 0.25, b_1 = 1, q = 0.6, h_1 = 0.7, \rho_1 = 1, \beta_1 = 1, d_2 = 0.9, \delta_2 = 0.03, b_2 = 0.4, \rho_2 = 0.9, \beta_2 = 0.9, h_2 = 0.5, \epsilon = 0.5, \alpha_2 = 0.7$.

An important question we can answer numerically is how far from the limit model we can see the evolutionary suicide. To answer this question we use the method of equilibrium continuation. The idea is to start from a parameter value, in this case $\alpha_1 = 0$, for which a solution of (16) is known. Then, to look for the closest solution of (16) with a small increase in α. This can be perform with the Matemathica command FindRoot. In particularly, we are interested in continue the fold bifurcation point where evolutionary suicide occurs, that we have analysed in the limit model with $h_2 \neq 0$. To this end, we need to add another equation and another unknown to (16). We need to find c_1 such that the determinant of the Jacobian matrix evaluated at the internal equilibrium is equal to zero. Then, we check if the point found is exactly a fold bifurcation point by controlly that there is a real eigenvalue equal to zero. The result is shown in Fig.30. The

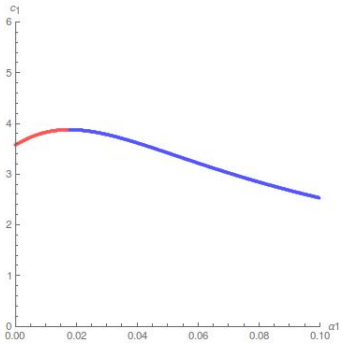

Figure 30: Value of c_1 where the fold bifurcation occurs with negative selection gradient as function of α_1. In the red part we still have evolutionary suicide. In the blue part both equilibria close to the fold bifurcation point are unstable. $d_1 = 0.1, \delta_1 = 0.25, b_1 = 1, q = 0.6, h_1 = 1, \rho_1 = 1, \beta_1 = 1, c_2 = 2.06, d_2 = 0.9, \delta_2 = 0.01, b_2 = 0.4, \rho_2 = 0.9, \beta_2 = 0.9, h_2 = 0.5, \epsilon = 0.5, \alpha_2 = 0.7$.

system undergoes into a fold-Hopf bifurcation for really small value of α_1. With MatCont we can get more information about the bifurcation. We can see in Fig.31 how the fold-Hopf (ZH) bifurcation arises when the Hopf bifurcation line intersects tangentially the fold one. Moreover, MatCont returns the coefficients of the normal form. In this case $s = 1$ and $\theta = 5.117328e - 02$, with $c_1 = 3.866959$ and $\alpha_1 = 0.017902$. For the equations of the normal form and its analytical

study see Kuznetsov (1998), p.337. Moreover, in Fig. 8.13 at p.339 we find the bifurcation diagram of the truncated normal form given that $s = 1$ and $\theta > 0$. Following Kuznetsov analysis, we can sketch the qualitative behaviour of solutions close to the bifurcation point. In this case the Hopf bifurcation is a subcritical one. We can identify four regions close to the fold-Hopf bifurcation (Fig.32). For the names of equilibria in three dimensional space see Figure 4. in [13]. In region 2 are present a stable focus-node and a saddle focus. When we go from region 2 to region 1 they collide in the fold bifurcation. In region 1 there are no internal equilibria, solutions in region 1 converge to the boundary equilibrium $(0, \bar{n}_2, \bar{p})$ that is stable since $c_2 < \bar{c}_2$. When we move from region 2 to region 3 the stable focus-node remains stable and the saddle-focus becomes an unstable focus-node trough the Hopf bifurcation. An unstable limit cycle generates from the subcritical Hopf bifurcation and stays present in region 3. From region 3 to region 4 the unstable cycle shrinks on the stable focus-node that loses stability and becomes a saddle focus. From region 4 to region 1 the saddle-focus and the unstable focus-node undergo through the fold bifurcation and, again, the internal equilibria disappear. These transitions can be observed in the numerical plot of the equilibria in a neighbourhood of the bifurcation point (Fig.33). In the left panel α_1 is slightly less than the fold-Hopf bifurcation value. Close to the fold bifurcation we are in region 2. Thus, we see the fold bifurcation between the stable focus-node and the saddle-focus. When c_1 increases we are going from region 2 to region 3, therefore the focus-node remains stable. In the right panel of Fig.33, α_1 is slightly above the fold-Hopf bifurcation value. Close to the fold bifurcation we are in region 4 and both the equilibria are unstable. By increasing c_1, we move from region 4 to region 3 and the saddle focus becomes a stable focus-node (green line on the upper branch of equilibria). Moreover, the selection gradient is still negative at the stable equilibria and there are not other internal attractor. The boundary equilibrium $(0, \bar{n}_2, \bar{p})$ is the only stable one in the the neighbourhood of the fold-Hopf bifurcation. This implies that evolutionary suicide still happens for value of α_1 slightly larger than the fold-Hopf bifurcation value. The difference is that in this case the evolutionary suicide happens because of a subcritical Hopf bifurcation rather than a fold one as before. This behaviour continues for the small range of α_1 where the Hopf bifurcation line remains above the fold bifurcation line. After that the two branches of equilibria are always unstable. We conclude that the limit value of α_1 for the evolutionary suicide is not the one where the fold-Hopf bifurcation happens but it is slightly larger.

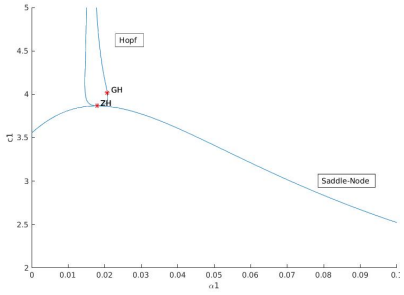

Figure 31: Fold-Hopf bifurcation (ZH) on the fold bifurcation line. The Hopf bifurcation is supercritical on the right branch of the Hopf bifurcation line above the generalized Hopf bifurcation point GH. $d_1 = 0.1, \delta_1 = 0.25, b_1 = 1, q = 0.6, h_1 = 1, \rho_1 = 1, \beta_1 = 1, c_2 = 2.06, d_2 = 0.9, \delta_2 = 0.01, b_2 = 0.4, \rho_2 = 0.9, \beta_2 = 0.9, h_2 = 0.5, \epsilon = 0.5, \alpha_2 = 0.7$. ZH=Zero-Hopf bifurcation (of fold-Hopf), GH=Generalized Hopf bifurcation.

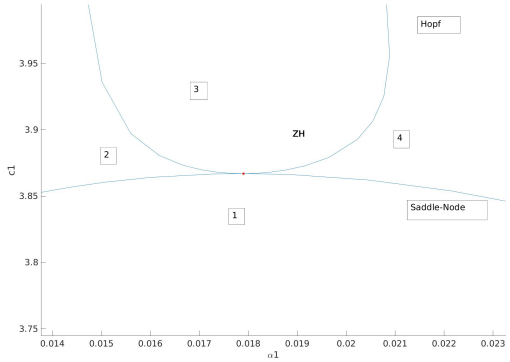

Figure 32: Neighbourhood of the fold-Hopf bifurcation. $d_1 = 0.1, \delta_1 = 0.25, b_1 = 1, q = 0.6, h_1 = 1, \rho_1 = 1, \beta_1 = 1, c_2 = 2.06, d_2 = 0.9, \delta_2 = 0.01, b_2 = 0.4, \rho_2 = 0.9, \beta_2 = 0.9, h_2 = 0.5, \epsilon = 0.5, \alpha_2 = 0.7$. ZH=Zero-Hopf bifurcation.

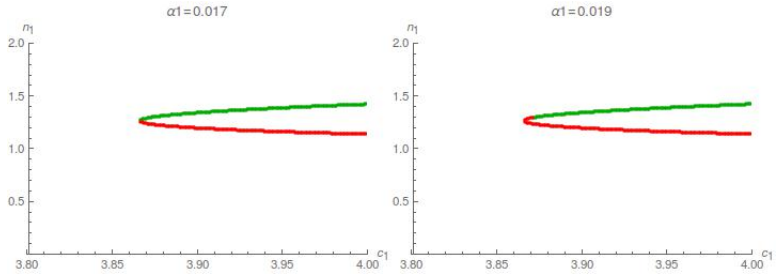

Figure 33: Internal equilibria close to the fold-Hopf bifurcation. Green dots for stable equilibria, red dots for unstable equilibria. $d_1 = 0.1, \delta_1 = 0.25, b_1 = 1, q = 0.6, h_1 = 1, \rho_1 = 1, \beta_1 = 1, c_2 = 2.06, d_2 = 0.9, \delta_2 = 0.01, b_2 = 0.4, \rho_2 = 0.9, \beta_2 = 0.9, h_2 = 0.5, \epsilon = 0.5, \alpha_2 = 0.7$.

3.2 Continuation of Matsuda and Abrams' model

In this paragraph we want to use the methods discussed in the previous paragraph to continue Matsuda and Abrams' model for positive values of α_1. We start from the simple case with $h_2 = 0$ that showed quantitatively the same results as Matsuda and Abrams' model. Then, we use the method of equilibria continuation to understand which is the range of α_1 where the model shows evolutionary suicide.

The stability conditions of the boundary equilibria are the same as the general full model. The only exception is that the Hopf bifurcation in the (n_2, p)-plane does not occurs. The equilibrium $(0, \bar{n}_2, \bar{p})$ is stable in the (n_2, p)-plane wherever it is positive. As can be seen in Fig.34 there is not upper bound of the light yellow region where $(0, \bar{n}_2, \bar{p})$ is stable.

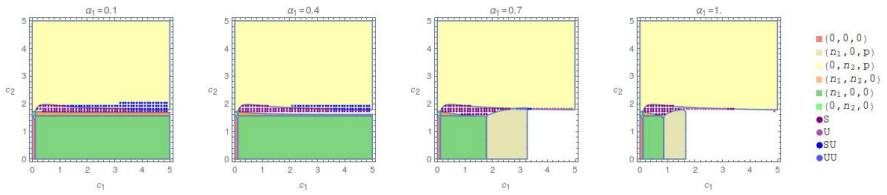

Figure 34: Stability regions of boundary equilibria and existence regions of internal equilibria. $d_1 = 0.1, \delta_1 = 0.25, b_1 = 1, \rho_1 = 1, \beta_1 = 1, h_1 = 1, d_2 = 0.9, \delta_2 = 0.01, b_2 = 0.4, \rho_2 = 0.9, \beta_2 = 0.9, \alpha_2 = 0.6, \epsilon = 0.5, q = 0.9$.

To perform the equilibrium continuation, we start from $\alpha_1 = 0$ and the same parameter set (8) as in Fig.7 with $c_2 = 1.95415$. We use MatCont to continue the fold bifurcation point for increasing α_1. Results are shown in the left panel of Fig.35. We can also plot with Mathematica the number of internal equilibria and the stability region of $(0, \bar{n}_2, \bar{p})$, the only stable boundary equilibrium for this choice of c_2, in the (α_1, c_1)-plane. Results are in the right panel of Fig.35. As

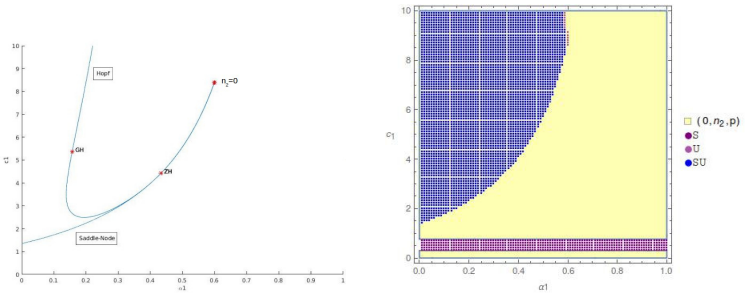

Figure 35: In the left panel, numerical continuation of the fold bifurcation point where evolutionary suicide occurs for $\alpha_1 > 0$ and $h_2 = 0$. In the right panel, existence regions of internal equilibria and stability regions of boundary equilibria in the (α_1, c_1)-plane. $d_1 = 0.1, \delta_1 = 0.25, b_1 = 1, \rho_1 = 1, \beta_1 = 1, h_1 = 1, d_2 = 0.9, \delta_2 = 0.01, b_2 = 0.4, \rho_2 = 0.9, \beta_2 = 0.9, \alpha_2 = 0.6, \epsilon = 0.5, q = 0.9$.

before, the Hopf bifurcation is a subcritical one. The peculiarity here is that the Hopf bifurcation line and fold one are numerically indistinguishable after the fold-Hopf bifurcation. As discussed in the previous paragraph, the closeness of the two lines implies that evolutionary suicide occurs also after the fold-Hopf bifurcation through the subcritical Hopf bifurcation. Unfortunately, the numerical overlapping of the two lines makes the analysis of the bifurcation that happens when $n_2 = 0$ difficult. Understanding the dynamics close to this bifurcation point would require deeper studies, beyond the porpoises of this work. However, we can conclude that the limit value for α_1 is considerably large, making Matsuda and Abrams' conclusion solid for this extension of the model.

Results

The aim of this thesis was to investigate the conditions and the permanence of evolutionary suicide in a two-prey-one-predator model with Holling type II predator functional response. When we analysed the model with $\alpha_1 = h_2 = 0$ we reproduced qualitatively and quantitatively same results of Matsuda and Abrams model. We showed that even with high predator density an high asymptotic value of the birth rate $B(c)$ can prevent the evolutionary suicide to occur.

In the case $\alpha_1 = 0$ and $h_2 \neq 0$ a supercritical Hopf bifurcation may occurs in the (n_2, p)-plane. We studied how the shape of the existence and stability region of the internal equilibria influences the evolutionary behaviour. In Fig.13 we notice that for low values of the prey competition rate δ_1 is possible that evolutionary suicide occurs on a limit cycle fold bifurcation. While for high values of δ_1 evolutionary suicide may only occur on equilibria bifurcation. In the critical function analysis on the birth rate as function of the foraging effort ($B(c)$) we noticed that the crucial role for evolutionary suicide is played by the slope of $B(c)$ at the fold bifurcation point. If this slope is to high natural selection increase the foraging, rescuing the population from evolutionary suicide.

In the analysis of the full model we showed the solidity of Matsuda and Abrams model with the assumption $h_2 = 0$. An interesting continuation of this work would be to analyses deeper the transition from $h_2 = 0$ to positive value of h_2 where evolutionary suicide disappears for very small α_1.

References

[1] Abrams, P.A., Matsuda, H. (1993). Effects of adaptive predatory and anti-predator behaviour in a two-prey-one-predator system. *Evol. Ecol. 7*, 312-326.

[2] Britton, N.F., (2003).*Essential Mathematica Biology*, Springer-Verlag London.

[3] Diekmann, O. (2003). A beginner's guide to adaptive dynamics. *Banach Center Publ. 63*, 47-86.

[4] Ferrière, R. (2000). Adaptive responses to environmental threats: evolutionary suicide, insurance, and rescue. *Options* Spring 2000, IIASA, Laxenburg, Austria, 12-16.

[5] Ferrière, Régis, Dieckmann, Ulf, and Couvet, Denis, eds. *Evolutionary Conservation Biology.* Cambridge, GB: Cambridge University Press, 2004. Copyright © 2004. Cambridge University Press. All rights reserved.

[6] Geritz, S.A.H., Kisdi, É, Meszéna, G., Metz, J.A.J. (1998). Evolutionarily singular strategies and the adaptive growth and branching of the evolutionary tree. *Evol. Ecol. 12*, 35-37.

[7] Gyllenberg, M., Parvinen, K. (2001). Necessary and sufficient consitions for evolutionary suicide. *Bulletin of Mathematical Biology 63*, 981–993.

[8] Gyllenberg, M., Parvinen, K., Dieckmann, U. (2002). Evolutionary suicide and evolution of dispersal in structured metapopulations. *J. Math. Biol. 45*, 79-105.

[9] Hardin, G. (1968). The tragedy of the commons. *Science 162*, 1243-1248.

[10] Kuznetsov, Y. (1998). *Elements of Applied Bifurcation Theory*, Secaucus, US: Springer.

[11] Matsuda, H., Abrams, P.A. (1994). Timid consumers: self-exinction due to adaptive change in foraging and anti-predator effort. *Theor. Popul. Biol. 45,* 76-91.

[12] Parvinen, K., (2005). Evolutionary suicide. *Acta Biotheoretica 53*, Issue 3, 241-264.

[13] Scolharpedia.
`www.scholarpedia.org/article/Equilibrium#Three-Dimensional_Space`

Acknowledgement

I want to extend my heartfelt thanks to Éva Kisdi for her inestimable support. Thanks also to Stefan Geritz for reviewing my thesis and to Francesca Scarabel for introducing me to MatCont. I am grateful to Mats Gyllenberg and to the whole Biomathematics Research Group for showing me what it means to do high-quality mathematical research and to make contributions to the international scientific community.

Thanks to my parents and my family for all the love and happiness that my life is made of.

Thanks to Marta for filling my days with laughter.

Thanks to Brittany for making me feel at home in Finland.

Thanks to Thomas, Marika, and Anita for remaining my friends through all the stress of the past two months.

Lastly, thanks to Greta, Antonietta, Ilaria, Jack, Fra, and Gaya for being my steady support throughout the years, despite distance and all the complications of life.